Explicit Computation of 4-point Correlators in Chern-Simons Matter Theory and Verification of Bosonisation Dualities

A Thesis

submitted to

Indian Institute of Science Education and Research Pune

in partial fulfillment of the requirements for the

BS-MS Dual Degree Programme

by

Umesh Sow

Indian Institute of Science Education and Research Pune
Dr. Homi Bhabha Road,
Pashan, Pune 411008, INDIA. April, 2024

Supervisor: Dr. Sachin Jain

Certificate

This is to certify that this dissertation entitled "Explicit Computation of 4-point Correlators in Chern-Simons Matter Theory and Verification of Bosonisation Dualities" towards the partial fulfilment of the BS-MS dual degree programme at the Indian Institute of Science Education and Research, Pune represents study/work carried out by Umesh Sow at Indian Institute of Science Education and Research under the supervision of Dr. Sachin Jain, Associate Professor, Department of Physics, during the academic year 2023-2024.

Sachin Jain

Dr. Sachin Jain

Committee:

Dr. Sachin Jain

Dr. Arun M. Thalapillil

This thesis is dedicated to my parents.

Declaration

I hereby declare that the matter embodied in the report entitled "Explicit Computation of 4-point Correlators in Chern-Simons Matter Theory and Verification of Bosonisation Dualities" are the results of the work carried out by me at the Department of Physics, Indian Institute of Science Education and Research (IISER), Pune, under the supervision of Dr. Sachin Jain and the same has not been submitted elsewhere for any other degree. Wherever others contribute, every effort is made to indicate this clearly, with due reference to the literature and acknowledgement of collaborative research and discussions.

Umesh Sow

Umesh Sow

Acknowledgments

I extend my gratitude to my supervisor, Dr. Sachin Jain, for his invaluable mentorship throughout this journey. His expertise and encouragement have been instrumental in shaping my research and fostering my personal and professional growth. I am equally indebted to Dr. Arun M. Thalapillil, the expert of this project work, whose invaluable feedback have greatly enhanced the quality and depth of my work.

I extend my sincere appreciation to my esteemed colleague, K. S. Dhruva, for the fruitful discussions and collaborations throughout this endeavor. I am profoundly grateful to my dear friends for their company in my tough times.

It will never suffice to appreciate the sacrifices, emotions and mental support I gain from my Maa-Baba, and Bordi-Chordi. Their unconditional love, support, and encouragement keep me moving forward.

I am grateful to Virat Kohli, who has always been a great source of motivation and dedication in my academic life. I would also like to thank Arijit Singh, without whose melodious voice, this academic journey would not have been that smooth.

Abstract

Chern-Simons theory is a special class of Conformal Field Theory. It possesses various interesting duality relations. These relations, or more accurately, these bosonisation duality relations connect the correlators of two different theory, namely the free fermionic Chern-Simons theory and critical bosonic Chern-Simons theory. These two theories are dual to each other. The correlators in these theories are calculated in the large N limit, up to all orders at the t' Hooft coupling. These expressions for the correlators can be derived from the free theories. Here, the verification of such duality relations are performed.

Contents

Abstract **xi**

List of Figures **xv**

1 Introduction **1**

2 Preliminaries **5**

2.1 Chern-Simons Matter Theory 5

2.2 Lagrangian 5

2.3 Feynman Rules 7

3 Background and Establishment **9**

3.1 CFT Correlators 9

3.2 Dual Theories 11

3.3 Conjectured Bosonisation Dualities 12

3.4 Verifying Bosonisation Dualities 14

4 Formalism **15**

4.1 Working Regime 15

4.2 Computation Method 18

4.3 Key Calculations from Existing Literature 25

5 Computation and Analysis 29

5.1 $\langle TJJ \rangle$ . . . 29

5.2 $\langle JJ\mathcal{O}\mathcal{O} \rangle$ . . . 31

5.3 $\langle JJJJ \rangle$ . . . 32

5.4 T Exact Vertex . . . 33

5.5 $\langle TJJ\mathcal{O} \rangle$ . . . 38

5.6 $\langle \mathcal{O}\mathcal{O}\mathcal{O}\mathcal{O}\mathcal{O} \rangle$ . . . 42

6 Results and Discussions 45

6.1 Results . . . 45

6.2 Discussions . . . 47

7 Conclusion 49

Bibliography 51

Appendices 55

A Polar Integrals 57

B 1-loop Calculation Simplifications 59

List of Figures

3.1 Dual Theories 12

4.1 Exact Vertex Depiction 18

4.2 Box Diagrams and Ladder Diagrams 19

4.3 Ladder Diagram Breakdown 19

4.4 Effective Vertex 20

4.5 4-point Tree Level 23

4.6 4-point Vertex Correction 24

4.7 4-point Propagator Self Energy 24

4.8 4-point Ladder Diagrams 25

5.1 The Tree Level 2-point diagram of the $\mathcal{O}$ Operator 42

5.2 The Tree Level 5-point diagram of the $\mathcal{O}$ Operator 43

Chapter 1

Introduction

Quantum field theory (QFT) is a fundamental concept within theoretical physics, combining quantum mechanics and special relativity to elucidate the actions of particles and fields. Its utility extends across a broad spectrum, aiding in our comprehension of how matter and forces function in the cosmos. But yet this is not the full story. There has been made a lot of attempt in combining QFT with general relativity (GR) aiming for a grand unified theory (GUT), describing all the fundamental forces of nature. And, string theory remains the most promising candidate for this. Here, comes Conformal Field Theory (CFT) as a gateway to string theory. CFT is a class of QFT, which maintain the angles relying on in the system but not the distances. It has an vast application in the realm of theoretical physics. One such example of CFT is the Chern-Simons (CS) matter Theory. (see [1], [2], [3])

Working with quantum field theory (QFT) entails comprehending the basic laws of the universe, and it involves resolving intricate scenarios that present challenging analytical problems. In such instances, perturbative QFT has been greatly valuable for making approximate calculations and predictions regarding physical occurrences. This approach of perturbation is particularly useful for systems where the exact solutions to the quantum field equations are extremely complex or impossible to obtain. But the perturbation technique looses much of its functionality when it comes to the cases of strongly coupled systems. Non-perturbative techniques are to be taken in such scenarios. Currently, we are working in the CS matter theory. An intriguing aspect of CS matter theory is the ability to extend perturbative techniques to address even strong couplings. (see [4], [5], [6], [7])

Chern-Simons (CS) theory represents a 3-dimensional topological quantum field theory. This theory refers to the coupling of CS theory with matter fields, such as fermions or scalars. CS theory exhibits numerous fascinating characteristics and holds a prominent position in multiple realms of theoretical physics and mathematics. Its mathematical and physical importance remains a vibrant field of study, intertwined with leading-edge subjects across various domains of contemporary physics. (see [8], [9])

Moreover, three-dimensional CS matter theory is exactly solvable. It is a basic class of a non-trivial CFT, and it could thus be used to study various phenomena, such as, strong-weak dualities and the AdS/CFT correspondence. It also has many applications in dualities. For instance, the free fermionic theory coupled with CS theory is dual to critical bosonic theory (it is a bosonic theory aimed to study the system at the critical points, namely Wilson-Fischer fixed point) coupled to CS theory; this is known as bosonisation duality. These kinds of theories are named quasi fermionic theories. Thus, the correlators in these theories are also related by a few interesting relations. (see [2], [10], [11]).

Correlation functions within CFT play a vital role as mathematical instruments which are used to calculate diverse physical parameters. They offer understanding into how fields behave at distinct spatial locations and are fundamental for grasping the characteristics of CFTs. Interpreting correlation functions in CFT entails examining the connections among various operators and their impacts on the system, revealing insights into the theory's fundamental physics and structure.

In this project work, we want to explicitly compute such few correlators. The computation in CFT has been mostly explored in position space. We have done our calculations in momentum space. There can be a lot of symmetries addressed in momentum space which simplify the theory to a considerate level but is not easily accessible in position space. However, the calculations for 3-point or 4-point correlators even in momentum space are quite intricate, so we will transition to a region where all external momenta are aligned with the z-component, making the calculation easier. Additionally, we employ the light-cone gauge and other certain strategies that facilitate the task and make it more manageable. Furthermore, we dedicate some time to calculate a few correlators using a covariant approach in a perturbative manner. (see [2], [12], [13])

Subsequently, we move forward with one of our primary objectives. We utilize a few previously computed correlators from the literature and direct our calculations towards the explicit proof of bosonisation dualities conjectured in CS matter theories. ([12], [13]) These dualities provide a powerful tool for understanding the dynamics of these systems and for deriving new results. They are effective for addressing conformal field theories in three dimensions and can also be applied to investigate thermal correlators in large N CS matter theories.

This thesis is organised as follows. In Chapter 2, titled Preliminaries, we introduce fundamental concepts crucial for understanding the entire narrative and specific calculations. These concepts serve as the foundational principles essential for the theory and the ongoing progress of this project. Chapter 3, Background and Establishment, offers a concise discussion to contextualize the problem and enhance comprehension. It presents various aspects and the underlying purpose of the completed work. Chapter 4, Formalism, delves into the specific assumptions and methodologies employed to address the problem of interest. The strategies outlined in this chapter prove beneficial in simplifying complex computations that would otherwise be daunting. Chapter 5, Computation and Analysis, details the methodology for computing correlators and relevant calculations. Chapter 6, Results and Discussions summarizes the noteworthy results obtained, accompanied by discussions on these outcomes. Finally, Chapter 7 serves as the conclusion, summarizing the overall progress of the project and briefly outlining potential future directions.

Chapter 2

Preliminaries

2.1. Chern-Simons Matter Theory

Chern-Simons theory is a special class of CFT. It provides exact solvability and a few applications of duality, which make this theory interesting. In general, in 3 or higher dimensions, computation work becomes very cumbersome. So, we proceed with 3-dimensional Chern-Simons Matter Theory.

2.2. Lagrangian

The action of the CS theory is proportional to the integral of the Chern-Simons 3-form, which is a topological invariant of the gauge field, which means its values are quantized and not affected by small perturbations/ deformations of the spacetime. The Lagrangian (Euclidean) for the abelian CS theory is,

$$\begin{aligned} \mathcal{L}_{\text{CS}} &= -\frac{i\kappa}{4\pi} Tr(AdA) \\ &= -\frac{i\kappa}{8\pi} \epsilon^{\mu\nu\rho} A^a_\mu \partial_\nu A^a_\rho \end{aligned} \tag{2.1}$$

Here, A is the gauge field, κ is the coupling constant known as Chern-Simons level.

The Lagrangian (Euclidean) for the non-abelian CS theory with gauge group SU(N) in fundamental representation is,

$$
\begin{aligned}
\mathcal{L}_{\text{CS}} &= -\frac{i\kappa}{4\pi} Tr(AdA + \frac{1}{3} f^{abc} A^3) \\
&= -\frac{i\kappa}{8\pi} \epsilon^{\mu\nu\rho} \left[A^a_\mu \partial_\nu A^a_\rho + \frac{1}{3} f^{abc} A^a_\mu A^b_\nu A^c_\rho \right] \\
&= -\frac{iN}{8\pi\lambda} \epsilon^{\mu\nu\rho} \left[A^a_\mu \partial_\nu A^a_\rho + \frac{1}{3} f^{abc} A^a_\mu A^b_\nu A^c_\rho \right]
\end{aligned} \tag{2.2}
$$

Here, $\lambda = \frac{N}{\kappa}$ is the t' Hooft coupling. In the context of non-perturbative phenomena, where traditional perturbation theory does not apply, the 't Hooft coupling is used to quantify the strength of the interactions in the study of strongly interacting systems. Taking the limit $N \to \infty$, λt Hooft $\to \infty$ leads to significant physical implications. To put it simply, the 't Hooft coupling at infinity indicates a deep relationship between gauge theories and quantum gravity, implying that certain gauge theories can encompass gravity in higher-dimensional spacetime. This idea is crucial to the AdS/CFT correspondence, where lower-dimensional gauge theories are equivalent to higher-dimensional gravitational theories, offering valuable insights into quantum field theory and gravity interactions.

Now coming to CS matter theory, the Lagrangian (Euclidean) for the CS theory in SU(N) gauge group coupled with free fermionic field is given by,

$$
\mathcal{L} = -\frac{iN}{8\pi\lambda} \epsilon^{\mu\nu\rho} \left[A^a_\mu \partial_\nu A^a_\rho + \frac{1}{3} f^{abc} A^a_\mu A^b_\nu A^c_\rho \right] + i\bar{\psi} \not{D} \psi \qquad \text{(where, } D_\mu = \partial_\mu - igA_\mu)
$$

Similarly, the Lagrangian (Euclidean) for the 3-dimensional CS theory in SU(N) gauge group coupled with complex scalar field is given by,

$$
\mathcal{L} = -\frac{i\kappa}{8\pi} \epsilon^{\mu\nu\rho} \left[A^a_\mu \partial_\nu A^a_\rho + \frac{1}{3} f^{abc} A^a_\mu A^b_\nu A^c_\rho \right] + (D_\mu \phi)^\dagger (D^\mu \phi)
$$

Now it is very straight forward to fetch the feynman rules for the corresponding theories.

2.3. Feynman Rules

2.3.1. Free Fermionic Theory coupled with CS theory

The relevant rules for the CS theory with SU(N) gauge group coupled with free fermionic field are,

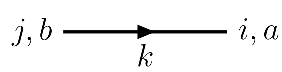

$$= i\frac{\not{k}}{k^2}\delta^i{}_j$$

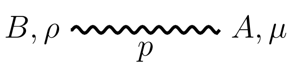

$$= -i\frac{4\pi}{\kappa}\epsilon^{\mu\nu\rho}\frac{p^\nu}{p^2}\delta^A{}_B$$

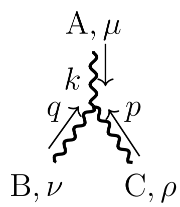

$$= \frac{\kappa}{12\pi}\epsilon^{\mu\nu\rho}f^{ABC}$$

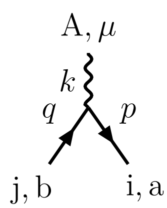

$$= ig\,(\gamma^\mu)^a{}_b(t^A)_{ij}$$

2.3.2. Scalar Theory coupled with CS theory

The relevant rules for the CS theory with SU(N) gauge group coupled with complex Scalar field are,

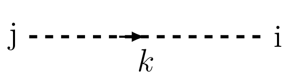

$$= \frac{i}{k^2 - m^2}\delta_{ij}$$

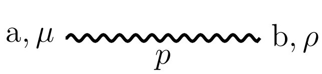

$$= -i\frac{4\pi}{\kappa}\epsilon_{\mu\nu\rho}\frac{p^\nu}{p^2}\delta_{ab}$$

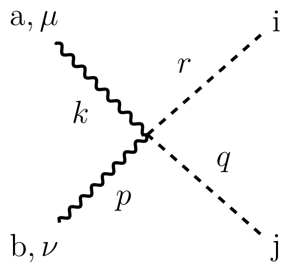

$$= ig^2\{t^a, t^b\}_{ij}$$

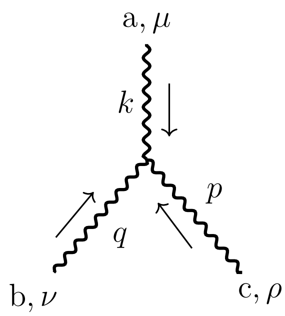

$$= \frac{i\kappa}{12\pi}\epsilon^{\mu\nu\rho} f^{abc}$$

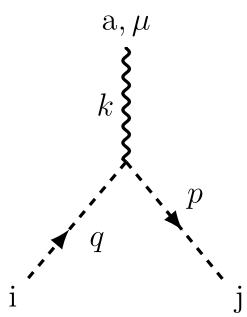

$$= ig(p+q)^\mu t^a_{ij}$$

Abbreviations

A few abbreviations that frequently appear in this thesis work, are gathered here for convenience.

$$\begin{aligned}
&\text{F.F.} \implies \text{Free Fermionic}\\
&\text{C.B.} \implies \text{Critical Bosonic}\\
&\text{Q.F.} \implies \text{Quasi Fermionic}\\
&\text{Odd} \implies \text{Parity Odd Contribution}
\end{aligned}$$

Chapter 3

Background and Establishment

In this chapter, we explain the objective of this project. Initially, we present background information to illustrate the complexity and scope of the issue being tackled. Next, we outline the approach to be taken, and finally, we detail the goals we aim to achieve.

3.1. CFT Correlators

In general terms, conformal field theories are Euclidean quantum field theories that possess a symmetry group that includes, along with Euclidean symmetries, local conformal transformations that maintain angles but not distances.

As a genuine quantum field theory, the condition of conformal invariance is highly restrictive. Specifically, due to its scale invariance, all particle-like excitations in the theory must be massless. (see [14])

Conformal field theories serve as simplified models for real interacting quantum field theories, they depict critical phenomena in two dimensions, and they hold a significant position in string theory, currently considered the leading contender for a unified theory encompassing all fundamental forces. (see [15])

There is a special class of CFT, the 'quasi fermionic' theories, which have a large N limit and the large N spectrum of operators consists of conserved high-spin currents and dimension two scalar operators. The theory of N free fermions coupled to $SU(N)_k$ Chern-Simons interactions and the theory of N critical bosons (or simply, free bosons, in our case) coupled to $SU(N)_k$ Chern-Simons interactions are example of such 'quasi fermionic' theories. (see [1])

In these theories, due to conformal invariance, the 3-point correlation function of conserved currents are constrained to contain at most three different conformal structures in the large N limit (see [16]),

$$\langle J_{s_1} J_{s_2} J_{s_3} \rangle = c_b \langle J_{s_1} J_{s_2} J_{s_3} \rangle_{\text{F.B.}} + c_f \langle J_{s_1} J_{s_2} J_{s_3} \rangle_{\text{F.F.}} + c_{\text{odd}} \langle J_{s_1} J_{s_2} J_{s_3} \rangle_{\text{odd}} \tag{3.1}$$

where, J is the conserved current and s_1, s_2 and s_3 are the associated spins, and c_b, c_f and c_{odd} are the corresponding coefficients. The F.F. term and F.B. term correspond to the correlators of the theory of free fermions and free bosons, respectively. The odd term is not generated by free theories and refers to independent conformally invariant contributions to the correlators that appear only in interacting theories. It is also important to mention that whenever, the conserved currents obey the 'triangle rule'(see [15], [17]),

$$s_i \leq s_j + s_k \qquad \text{(where, } \{i, j, k\} \quad \epsilon \quad \{1, 2, 3\}\text{)}$$

the odd term contribution is nonzero. But if the triangle rule is violated, that is,

$$s_i > s_j + s_k \qquad \text{(where, } \{i, j, k\} \quad \epsilon \quad \{1, 2, 3\}\text{)}$$

then, for conserved-current correlators, there is no parity-odd contribution. Now, if the slightly broken high-spin (SBHS) symmetry is imposed on these theories, in the large N limit, the 3-point correlators get further constrained to the following functional form,

$$\langle J_{s_1} J_{s_2} J_{s_3} \rangle = \frac{\tilde{N}}{1 + \tilde{\lambda}^2} \left[\langle J_{s_1} J_{s_2} J_{s_3} \rangle_{\text{F.B.}} + \tilde{\lambda}^2 \langle J_{s_1} J_{s_2} J_{s_3} \rangle_{\text{F.F.}} + \tilde{\lambda} \langle J_{s_1} J_{s_2} J_{s_3} \rangle_{\text{odd}} \right] \tag{3.2}$$

where, the notation is such that (as in [16]),

$$\tilde{N} = 2N\frac{sin(\pi\lambda)}{\pi\lambda} \qquad\qquad \tilde{\lambda} = \tan\frac{\pi\lambda}{2} \tag{3.3}$$

There is another interesting property of 3-point functions. If the spin of two conserved current are identical and the third one has an odd spin, then the correlator becomes zero. (see [1], [18])

$$\langle J_s J_s J_{s\prime}\rangle = 0 \qquad\qquad \text{(for } s\prime \text{ odd)}$$

3.2. Dual Theories

The previously mentioned examples of 'quasi fermionic' theories are dual to each other. In other words, in the large limit N, the theory of N free fermions coupled with CS theory with the gauge group $SU(N)_k$, also known as Free Fermionic (FF) theory is dual to the theory of N free bosons coupled with CS theory with the gauge group $SU(N)_k$, also known as Free Bosonic (FB) theory. (see [2])

Beginning with the free fermionic theory, introducing the CS coupling, $\tilde{\lambda}$, and then taking it to infinity (reaching the strong coupling limit $\lambda \to 1$) leads to the critical bosonic (Wilson-Fischer) theory. The corresponding bosonisation duality establishes a connection between free fermionic CS theories with strength $\tilde{\lambda}$ and critical bosonic theories with strength $\frac{1}{\tilde{\lambda}}$ coupled to CS. The bulk duals are represented by the type-B Vasiliev θ theories, which are characterized by $\theta \quad \epsilon[0, \pi/2]$. (see [2], [19])

The critical bosonic theory is an advanced and refined version of the free bosonic theory, which focuses on examining the system at critical junctures, specifically at the Wilson-Fischer fixed point. Vasiliev Type-B theories belong to a category of internally coherent gauge invariant nonlinear equations in the realm of higher-spin theory. Higher-spin theory, also known as higher-spin gravity, deals with field theories encompassing massless fields with spins exceeding two, such as the graviton. (see [20])

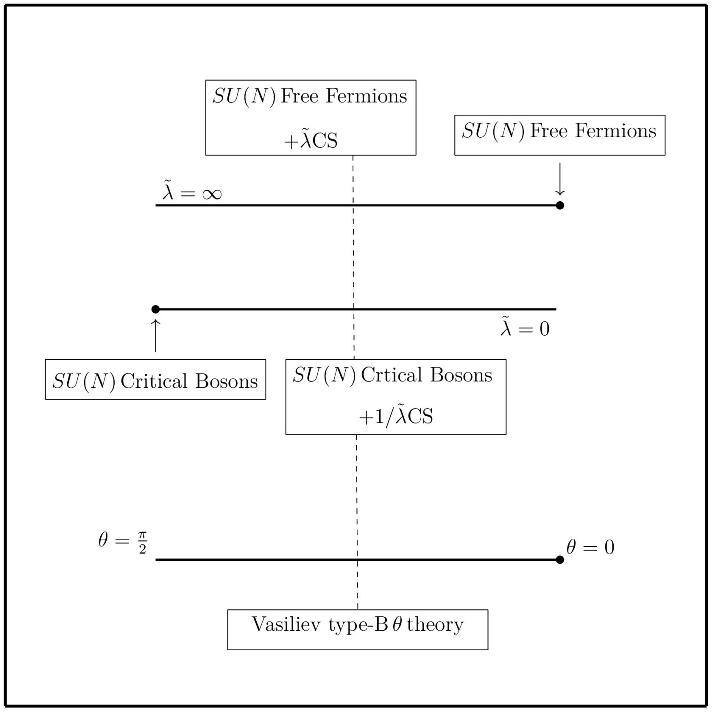

Figure 3.1: The Quasi Fermionic Theories: the Duality relations

3.3. Conjectured Bosonisation Dualities

As the free fermionic and critical bosonic theories are dual to each other, it is quite obvious that there might be some interesting relations between the theories. One of such relations hold the following mathematical form,

$$
\begin{aligned}
&X_{\mathbf{Q.F.}} = A(X_{\mathbf{F.F.}} + \tilde{\lambda} X_{\mathbf{Odd}} + \tilde{\lambda}^2 X_{\mathbf{C.B.}}) \\
&\epsilon \cdot (X_{\mathbf{F.F.}} - X_{\mathbf{C.B.}}) = \pm i X_{\mathbf{Odd}} \\
&\epsilon \cdot X_{\mathbf{F.F.\text{-}C.B.}} = \pm i X_{\mathbf{Odd}}
\end{aligned} \tag{3.4}
$$

where, X is some conserved-current correlator in the quasi fermionic theory and A denotes some overall normalization factor coefficient multiplied with the expression in the right. Besides, the F.F., C.B. and Odd terms represent the free fermionic, critical bosonic and parity-odd contributions. The F.F. and C.B. are the parity-even contributions. These bosonisation relation conveys that the parity-even contributions for some correlators in the quasi fermionic theories are related to the parity-odd contributions by a functional form. (see [1], [14]) And the transition is attained by following an abstract technique known as 'epsilon transformation' (E.T.). These duality relations can be found in [18].

These bosonisation duality relations already found to be obeyed for 3-point correlators, (for example TJJ, where T is the stress-energy tensor and J is the spin-1 current). [17] But it is also suggested that these duality relations also hold for 4-point correlators. Let us first introduce the epsilon transformation and then come back again to the duality relations.

3.3.1. Epsilon Transformation

This is a transformation method which converts a parity-even term into a parity-odd term and vice versa. It applies to the conserved currents (see, [17], [12], [13]). Epsilon transformation for the spinor-helicity variables can be written down as,

$$\epsilon \cdot X^{\mu\nu\alpha_1\cdots\alpha_n} = \frac{\epsilon^{(\mu ab}p_a}{p} X_b^{\nu)\alpha_1\cdots\alpha_n} \tag{3.5}$$

where, X is some correlator and p is the momenta associated with the operator inside the correlator and $\epsilon^{\mu ab}$ is the Levi-civita tensor and the conserved current operators are the ones associated with the μ and ν indices (here, in this depiction). Furthermore, it is crucial to emphasize that this transformation must be applied symmetrically to all conserved current operators within the correlator. The conserved current condition can be simply found as in [1],

$$\partial_\mu J^\mu{}_{\nu\cdots\rho} = 0 \tag{3.6}$$

Therefore, a clearer representation would be,

$$\begin{aligned} &\epsilon \cdot \langle X_1^\mu X_2^\nu X_3^\alpha \cdots \rangle \\ &= \frac{\epsilon^{\mu ab}p_{1a}}{p_1} \langle X_{1b} X_2^\nu X_3^\alpha \cdots \rangle + \frac{\epsilon^{\nu ab}p_{2a}}{p_2} \langle X_1^\mu X_{2\nu} X_3^\alpha \cdots \rangle + \frac{\epsilon^{\alpha ab}p_{3a}}{p_3} \langle X_1^\mu X_2^\nu X_{3\alpha} \cdots \rangle + \cdots \end{aligned} \tag{3.7}$$

3.4. Verifying Bosonisation Dualities

Now, we want to explicitly check the bosonisation dualities achieved by the epsilon transformation. But for that one needs to have the expression for the correlators, which is a cumbersome task to do. Hence, we first show the validity of this duality relation for the 3-point correlator $\langle TJJ \rangle$ ([16]), where this is relatively easy to visualize. Then, we move to check a few 4-poit correlators. We make use of some available expression for the correlators $\langle JJ\mathcal{O}\mathcal{O} \rangle$ and $\langle JJJJ \rangle$ ([2]). Besides, we try to compute $\langle TJJ\mathcal{O} \rangle$ and then verify the suggested relations.

Chapter 4

Formalism

In this section, we explore the general strategies used in computation and illustrate the techniques employed to obtain correlators.

4.1. Working Regime

Our goal is to derive the complete expression of correlators within a perturbative framework. However, obtaining the all-loop result for any correlator proves excessively intricate. Therefore, we focus on a simpler regime that allows for more manageable calculations. Here, we provide guidance on achieving this.

4.1.1. Light-Cone Gauge

To begin, we transition to the light-cone coordinates (Dirac coordinates) and then utilize the light-cone gauge. Light-cone coordinates has demonstrated its utility in intricate scenarios. ([21], [22]) In this context, the light-cone transformation for the Euclidean signature is defined as follows.

$$x^{\pm} = x_{\mp} = \frac{1}{\sqrt{2}}(x^1 \pm ix^2) \tag{4.1}$$

$$\begin{aligned} \text{In Cartesian coordinates,} \quad & ds^2 = (dx^1)^2 + (dx^2)^2 + (dx^3)^2 \\ \text{In Light-cone coordinates,} \quad & ds^2 = 2(dx^+)(dx^-) + (dx^3)^2 \end{aligned} \tag{4.2}$$

So, the metric in the light-cone gauge is given by,

$$g^{\mu\nu} = \begin{pmatrix} 0 & 1 & 0 \\ 1 & 0 & 0 \\ 0 & 0 & 1 \end{pmatrix} \tag{4.3}$$

Hence, it is quite obvious,

$$x_s^2 \equiv x_1^2 + x_2^2 = 2x^+x^- = 2x_+x_- \tag{4.4}$$

$$p^\pm = p_\mp = \frac{1}{\sqrt{2}}(p^1 \pm ip^2)$$

$$A^\pm = A_\mp = \frac{1}{\sqrt{2}}(A^1 \pm iA^2)$$

$$p_s^2 \equiv p_1^2 + p_2^2 = 2p^+p^- \tag{4.5}$$

Now, the light-cone gauge is defined as $A^+ = A_- = 0$, as previously used by [3], [23]. This is achieved using Wick rotation. This is a similar implication of light-cone gauge in the Euclidean signature coming directly from the standard light-cone gauge in the Lorentzian signature. It is crucial to notice that $A^+ = A_- = 0$ is achieved as an analytic continuation of the Lorentzian space, otherwise one could have obtained $A_+ = (A_-)^* = 0$. (see [3], [2]). This gauge fixing brings about substantial modifications to the Feynman rules of this theory. It eliminates the self-interactions of gluons and leads to a revised description of the gluon propagator, as follows,

$$\left\langle A_+^a(p)A_z^b(-q)\right\rangle = -\left\langle A_z^a(p)A_+^b(-q)\right\rangle = \frac{4\pi i}{k}\frac{1}{p^+} \times (2\pi)^3\delta(p-q)\delta^{ab} \tag{4.6}$$

It is very important to note here that, we will frequently be interchanging between (x^+, x^-, x^3) and (x^+, x^-, x^z), while, x^3 and x^z denotes the same. Moreover, $x^+ = x_-$, $x^- = x_+$ and $x^z = x_z$.

4.1.2. Collinear Perturbation Theory

While correlators provide valuable insights into the theory, their determination remains a challenging endeavor. However, as demonstrated by [2], [11], [24] and [25], it becomes feasible when computations are conducted within a framework where all external momenta align along the z-component. Therefore, we make use of the following simplification. For any external momenta, p,

$$\begin{aligned} p &= p_z = p^z \\ \implies p &= (0, 0, p_z) \end{aligned} \tag{4.7}$$

This approach, known as "collinear perturbation theory", has been previously employed to calculate two-, three-, and even four-point correlators of single-trace operators, with expressions being directly dependent on the 't Hooft coupling. A significant application of this method, which has motivated our work, can be found in [24], where this method of representing external momenta for deriving the expression for $\langle \mathcal{O}\mathcal{O}\mathcal{O}\mathcal{O} \rangle$ was first utilized (although later corrected by [25]). Additionally, in [11] a procedure has been outlined for calculating all n-point functions of the form, $\langle \mathcal{O}\mathcal{O}\mathcal{O}\mathcal{O} \cdots \rangle$ within the collinear regime (at leading order in 1/N).

It is essential to highlight that this regime of collinear momenta also influences the epsilon transformation method. For instance, directly from 3.7, it can be shown that,

$$\begin{aligned} \epsilon \cdot \langle X_1^\mu X_2^\nu X_3^\alpha \cdots \rangle &= \epsilon^{\mu z b} \operatorname{sgn}(p_1) \langle X_{1b} X_2^\nu X_3^\alpha \cdots \rangle \\ &\quad + \epsilon^{\nu z b} \operatorname{sgn}(p_2) \langle X_1^\mu X_{2\nu} X_3^\alpha \cdots \rangle + \epsilon^{\alpha z b} \operatorname{sgn}(p_3) \langle X_1^\mu X_2^\nu X_{3\alpha} \cdots \rangle + \cdots \end{aligned} \tag{4.8}$$

It is worth noticing that all the dependence on the explicit form of momentum associated with certain operators now has shifted only to the signature of the corresponding momenta. This is exciting as it simply transforms the complex expressions into just an overall summation of different correlators of different helicity combinations.

4.2. Computation Method

Within this segment, we provide a detailed guide on deriving the expressions for the desired correlators. Both approaches utilizing the 'exact' and 'free' (to be elaborated shortly) formulations of the vertices and propagators are discussed.

4.2.1. Computation with exact vertices and propagators

To obtain the complete expression for certain correlators up to all loops, the conventional approach involves adding successive 1-loop corrections, 2-loop corrections, and so forth, which can be exceedingly intricate and demanding. However, there exists a modification that can be used to ease the process, that is, reducing the number of diagrams that may contribute to the corrections. The 'free' vertices and 'free' propagators are now replaced by 'exact' vertices and 'exact' propagators (see [10], [2]). In this context, the term 'exact' vertex (or propagator) refers to the combination of the 'free' vertex (or propagator) with all loop contributions. This integration encompasses all vertex corrections and propagator self-energy corrections within the 'exact' expressions, simplifying the calculation process. Here, a simple depiction of the 'exact' vertex is shown,

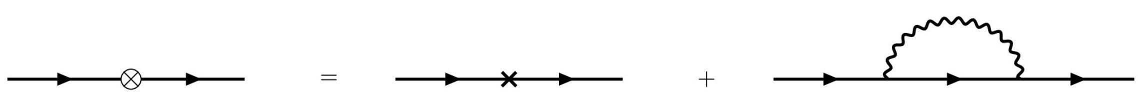

Figure 4.1: An illustration showcasing the exact vertices and free vertices. The diagram on the left featuring a circled cross represents the exact vertex, the middle diagram with a cross represents the free vertex, and the diagram on the right depicts the all-loop correction to the free vertex.

Given that our focus is on a 4-point correlator, we develop a methodology tailored specifically for 4-point correlators. Presently, the all-loop contributions solely focus on diagrams featuring a gauge propagator connecting any two non-adjacent sides of the correlators. As illustrated in [2], in the context of a 4-point correlator, for a certain alignment of operators at the vertex, the relevant diagrams can be categorized into 'box' diagrams and 'ladder' diagrams. Different configuration of operators result into different set of box digrams and ladder diagrams. Box diagrams correspond to the contributions at tree level, while ladder diagrams account for the all-loop contributions using 'exact' vertices and propagators. Ladder diagrams are presented as a collective sum of corrections. These are depicted in the following diagrams.

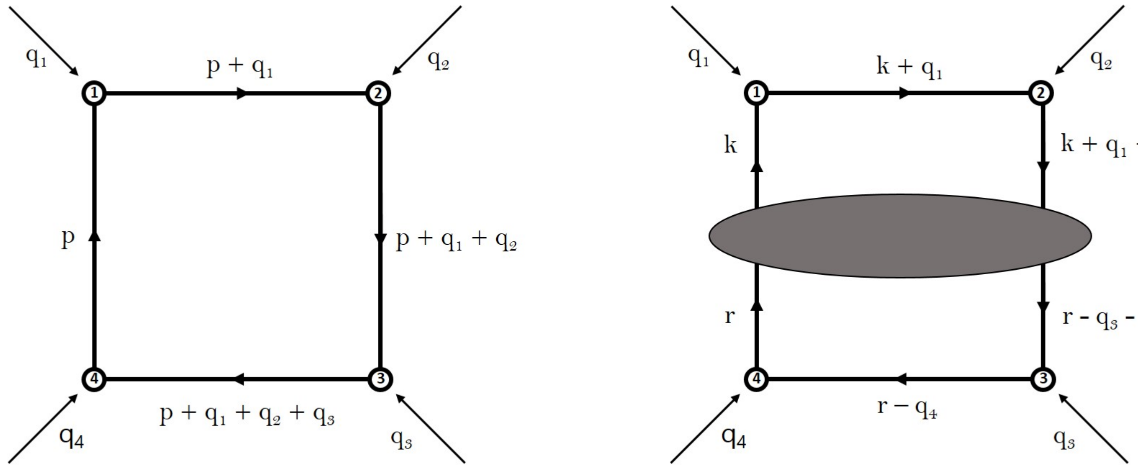

Figure 4.2: The diagram on the left is a box diagram, while the diagram on the right features a ladder diagram with a large blob in its center. (Image Credit: [2].) In these diagrams, the vertices labeled 1, 2, 3, and 4 represent four operators, and the propagator momenta are indicated as p in the box diagram and as r and k in the ladder diagram. The external momenta are represented as q_1,q_2,q_3, and q_4 respectively.

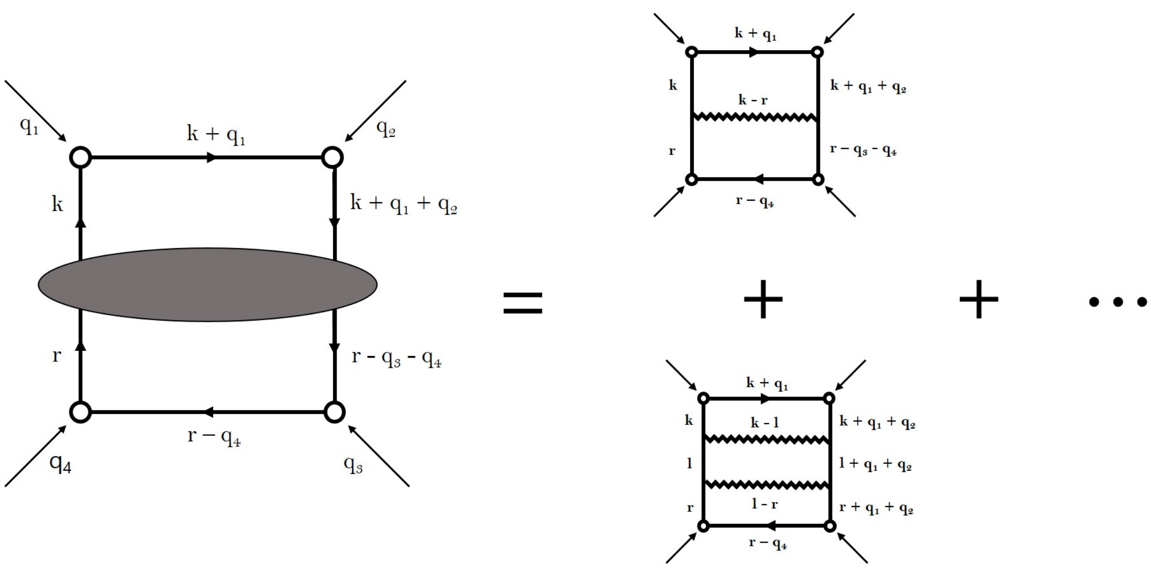

Figure 4.3: The ladder diagram, for a specific arrangement of operators at the vertices, consolidates all loop contributions into a unified 1-loop-like contribution. (Image Credit: [2].) Here, k, r and l represent the propagator momenta and q_1,q_2,q_3, and q_4 respectively represent the external momenta.

Moreover, the ladder diagrams can be visualized as illustrated in the figure, 4.3. For a clearer representation, the blob-like component in the ladder diagrams can be redefined as an 'effective vertex', signifying contributions from all loops. (see, figure 4.4.) Essentially, all loop corrections arising from gauge propagators connecting opposite sides can be summed linearly to create the impression of a single loop correction. These methods, previously employed with success by [2], are briefly outlined here to provide guidance for the research conducted in this project. Therefore, the comprehensive expression encompassing all loops can be derived as,

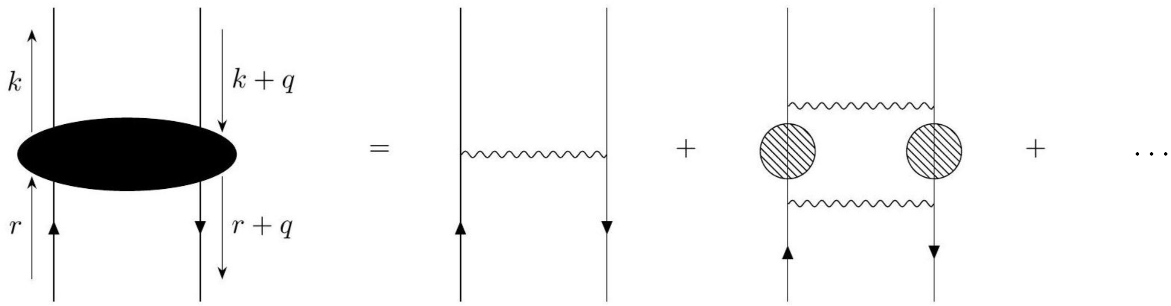

Figure 4.4: Effective vertex. (Image credit [2]). In this depiction, the blob-like element on the left signifies the effective vertex, while the right side illustrates loop contributions of all orders.

$$
\begin{aligned}
&-\int \frac{\mathrm{d}^3 r}{(2\pi)^3}\frac{\mathrm{d}^3 k}{(2\pi)^3}\,\mathrm{Tr}\left[\mathrm{S}\left(k+q_1+q_2\right)\mathcal{O}_2\ \mathrm{S}\left(k+q_1\right)\mathcal{O}_1\ \mathrm{S}(k)\gamma^\mu \mathrm{S}(r)\mathcal{O}_4\ \mathrm{S}\left(r-q_4\right)\mathcal{O}_3\right.\\
&\qquad\qquad \left.\mathrm{S}\left(r-q_3-q_4\right)\gamma^\nu\right]\mathrm{G}_{\mu\nu}(k-r) \qquad +\\
&-\int \frac{\mathrm{d}^3 r}{(2\pi)^3}\frac{\mathrm{d}^3 k}{(2\pi)^3}\frac{\mathrm{d}^3 l}{(2\pi)^3}\,\mathrm{Tr}\left[\mathrm{S}\left(k+q_1+q_2\right)\mathcal{O}_2\ \mathrm{S}\left(k+q_1\right)\mathcal{O}_1\ \mathrm{S}(k)\gamma^\mu \mathrm{S}(l)\gamma^\rho \mathrm{S}(r)\mathcal{O}_4\right.\\
&\qquad \left.\mathrm{S}\left(r-q_4\right)\mathcal{O}_3 \mathrm{S}\left(r-q_3-q_4\right)\gamma^\sigma \mathrm{S}\left(l+q_1+q_2\right)\gamma^\nu\right]\mathrm{G}_{\mu\nu}(k-l)\mathrm{G}_{\rho\sigma}(l-r)\\
&\qquad\qquad + \qquad \ldots
\end{aligned} \tag{4.9}
$$

where, the $\mathcal{O}$ and S represent the 'exact' vertices and the 'exact' propagators, with the subscripts indicating their respective positions. After using spinor indices and performing some algebraic manipulations, this expression can be reduced to,

$$
\begin{aligned}
= -\int \frac{\mathrm{d}^3 r}{(2\pi)^3}\frac{\mathrm{d}^3 k}{(2\pi)^3}&\left[\ \mathrm{S}\left(k+q_1+q_2\right)\mathcal{O}_2\ \mathrm{S}\left(k+q_1\right)\mathcal{O}_1\ \mathrm{S}(k)\right]_j^m \Gamma_{im}^{jn}\left(k, q_1+q_2, r\right)\\
&\left[\mathrm{S}(r)\mathcal{O}_4\ \mathrm{S}\left(r-q_4\right)\mathcal{O}_3\ \mathrm{S}\left(r-q_3-q_4\right)\right]_n^i
\end{aligned} \tag{4.10}
$$

Here, $\Gamma^{jn}_{im}(k,q,r)$ denotes the effective vertex, which is a complex equation involving various gamma matrices and summation of products of several propagators. Since we are operating within the collinear perturbation framework, the expression can be reformulated into a recursive Schwinger-Dyson equation and resolved using the techniques outlined in [26]. Upon transformation into a different basis, denoted as $\Gamma^{jn}_{im}(k,q,r)$ in accordance with [25], it emerges as a $2 \times 2 \times 2 \times 2$ matrix and can be represented as,

$$\Gamma^{jn}_{im}(k,q,r) = \Gamma_{AB}(k,q,r)\left(\gamma^{A}\right)^{n}_{m}\left(\gamma^{B}\right)^{j}_{i} \tag{4.11}$$

where $A, B \in \{+,-,3,I\}$, and $\gamma^{I} = \mathbf{1}_{2\times 2}$. This expression can be inverted as,

$$\Gamma_{AB}(k,q,r) = \frac{1}{4}\left(\gamma_{A}\right)^{m}_{n}\left(\gamma_{B}\right)^{i}_{j}\Gamma^{jn}_{im}(k,q,r) \tag{4.12}$$

Finally, we arrive at,

$$\begin{aligned} = -\int \frac{\mathrm{d}^3 r}{(2\pi)^3}\frac{\mathrm{d}^3 k}{(2\pi)^3}\,\mathrm{Tr}\Big[&\mathrm{S}\left(k+q_1+q_2\right)\mathcal{O}_2\ \mathrm{S}\left(k+q_1\right)\mathcal{O}_1\ \mathrm{S}(k)\gamma^{A}\ \mathrm{S}(r)\mathcal{O}_4 \\ &\mathrm{S}\left(r-q_4\right)\mathcal{O}_3\ \mathrm{S}\left(r-q_3-q_4\right)\gamma^{B}\Big]\,\Gamma_{AB}\left(k,q_1+q_2,r\right) \end{aligned} \tag{4.13}$$

The expressions for $\Gamma_{AB}(k,q,r)$ can be found in [2], appendix A.

At this point, it becomes evident that, for any 4-point correlator and a specific configuration of the operators at the vertices, given the exact expression for the corresponding operators and the propagators, one can obtain the explicit expression for that correlator in the large N limit up to all orders.

But the computation of 'exact' vertices is nevertheless an easier problem to tackle. Now we move to compute these kinds of vertices. It is worthwhile to mention that, using the techniques decribed in [10], the 'exact' vertex expressions for $\mathcal{O}$ and J operator have been computed.

4.2.2. Computation of Exact Vertices

The infinite tower of conserved current are denoted by, J_s ($\partial J_s = 0$). Their definition is provided by [3], [2]. We write down them here.

$$\begin{aligned} J_0 &= \bar{\psi}\psi \\ J_1^{\mu} &= i\bar{\psi}\gamma^{\mu}\psi \\ J_s^{\mu_1\mu_2\ldots\mu_s} &= \bar{\psi}\gamma^{(\mu_1}\mathcal{D}^{\mu_2}\ldots\mathcal{D}^{\mu_s)}\psi - (\text{ traces }) \end{aligned} \tag{4.14}$$

The concept of the exact vertex can be visualized as shown in Figure 4.1. With all computations conducted in the light-cone gauge and collinear perturbation regime, we can deduce the exact vertex in the following manner,

$$V^{\mu\nu}(p,q) = V_0^{\mu\nu}(p,q) + 2\pi i\lambda \int \frac{d^3k}{(2\pi)^3}\frac{\gamma^{[3|}S(k)V^{\mu\nu}(p,k)S(k-p)\gamma^{|+]}}{(q-k)^+} \tag{4.15}$$

where, $V^{\mu\nu}(q,p)$ and $V_0^{\mu\nu}(q,p)$ represents the exact vertex and free vertex with propagator momenta q and external momenta p and $S(k)$ represents the exact propagator with propagator momenta k. Moreover, the $(q-k)^+$ part signifies the gauge propagator. It is important to note that, both, the directions of the gauge propagator are considered. This methodology is derived from [10], where they have previously computed the exact vertex formulations for $\mathcal{O}$ (or J_0), J^+, and J^- ($J \equiv J_1$) operators.

Prior to delving into the resolution of this intricate equation, it is essential to pause and contemplate, aiming to introduce some simplifications. One notable simplification that can significantly reduce complexity stems from relations derived directly from light-cone coordinate algebra. This outcome is detailed in [3] and [10]. For a 2×2 matrix $A = a_\mu\gamma^\mu + a_I I$, it satisfies,

$$\gamma^{[3|}A\gamma^{|+]} = 2\left(a_I\gamma^+ - a_- I\right) \tag{4.16}$$

Now, the complicated numerator has only the relevant contributions from γ^- and I.

4.2.3. Computation with free vertices and propagators

As illustrated in 4.1.1, the comprehensive formulation for all-loop contributions involves intricate integral equations requiring gamma trace algebraic manipulations. Consequently, in some scenarios, the resulting expression becomes too unwieldy to handle, making it challenging to extract. In such cases, reverting to 'free' vertices and 'free' propagators becomes necessary to assess the loop contributions effectively. Therefore, we present the methodology for computing tree-level and 1-loop contributions for 4-point correlators using 'free' vertices and propagators, here.

The tree level diagrams for any 4-point correlator are given by,

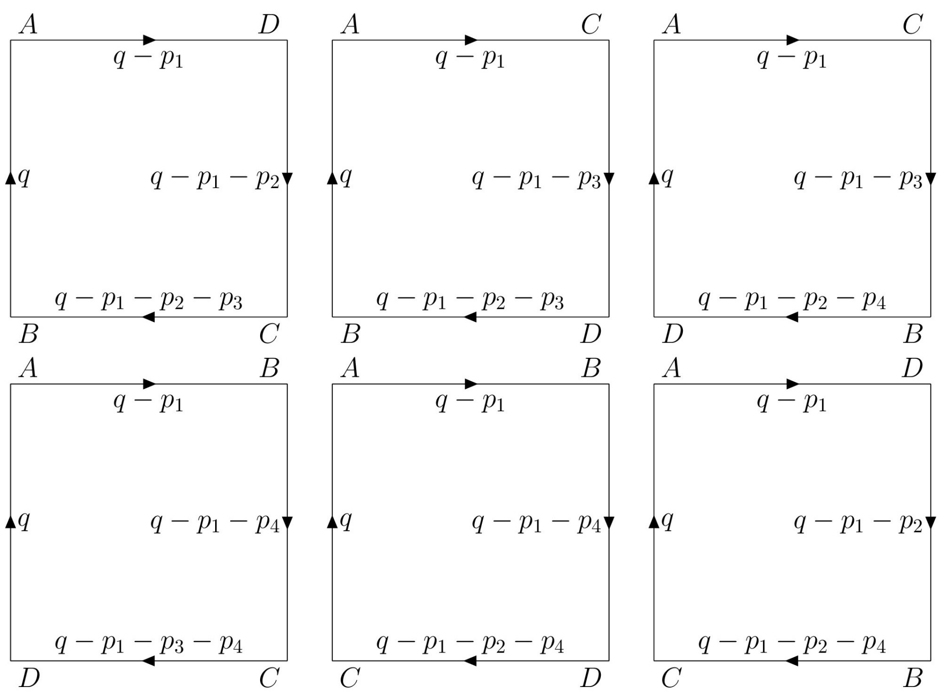

Figure 4.5: Where, A, B, C and D represent 4 operators and their corresponding external momenta are p_1, p_2, p_3 and p_4 respectively. The propagator momenta here are q. Moreover, the momentum conservation rule, i.e, $p_1 + p_2 + p_3 + p_4 = 0$ is in action.

At this point, it is quite essential to introduce concise and efficient notations to manage these intricate diagrams effectively. Therefore, we introduce,

$$q_i := q - P_i, \qquad k_i := k - P_i \qquad\qquad \text{and} \qquad P_i := \sum_{j=1}^{i} p_j \tag{4.17}$$

The 1-loop correction diagrams for the configuration (anti-clockwise) ABCDA (the first diagram in figure 4.5) are given below. The vertex correction diagrams are,

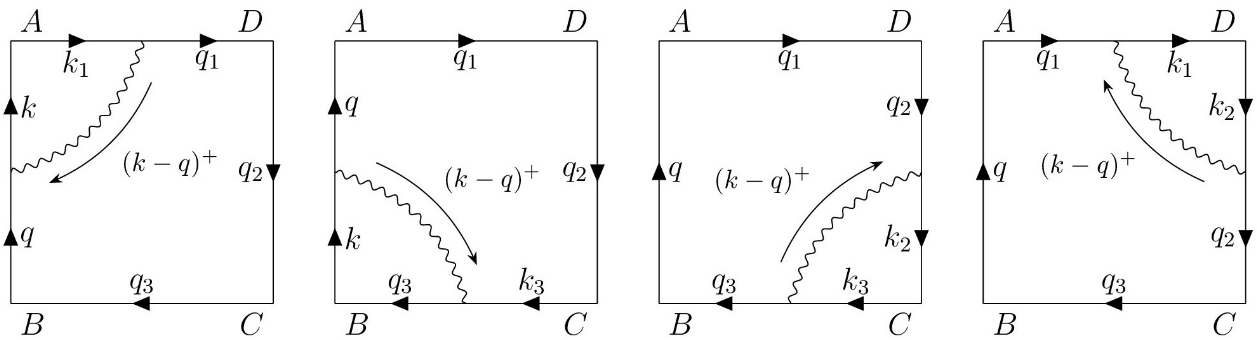

Figure 4.6: Vertex correction diagrams for a 4-point correlator.

The propagator self energy diagrams are,

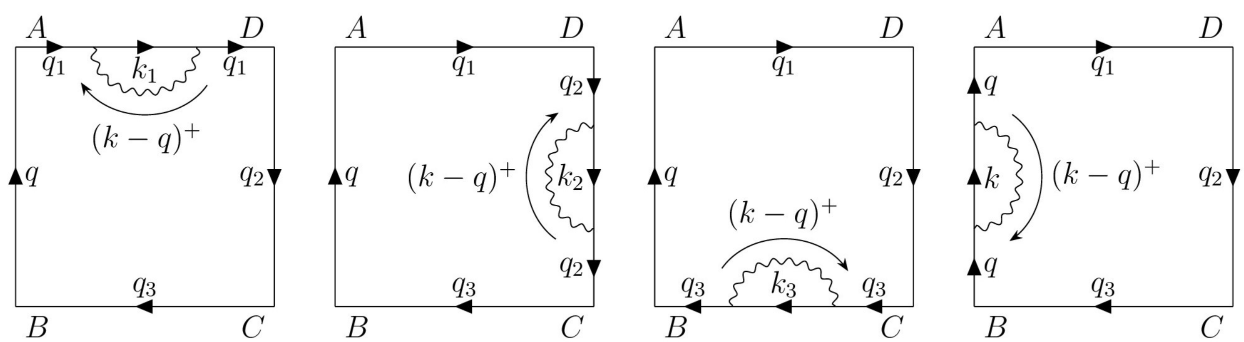

Figure 4.7: Propagator self energy diagrams for a 4-point correlator.

Previously, these two sets of diagrams were not taken into account for 'exact' vertices and propagators, but they play a significant role in this context. Now, turning to the ladder diagrams, which are also there in the 'free' formalism, it can be noticed that these diagrams are basically a gauge propagator connecting the opposite sides and cutting the 4-point box diagram into two symmetrical parts.

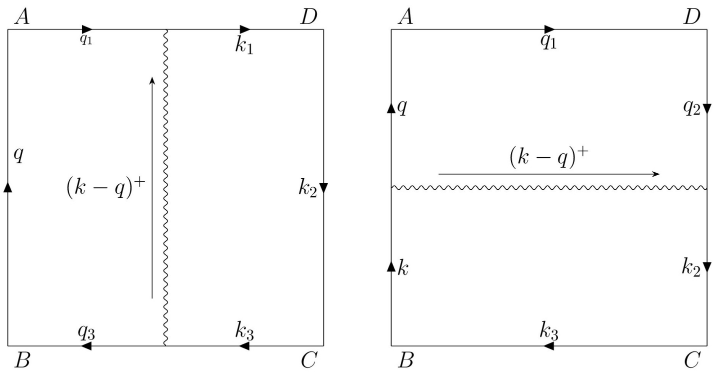

Figure 4.8: Ladder diagrams for a 4-point correlator.

So, it is pretty clear that, for a particular configuration of operators, a 4-point correlator demands 10 1-loop corrections and in total for any particular 4-point correaltor the total 1-loop corrections become 60!!

4.3. Key Calculations from Existing Literature

In this section, we gather all the available expressions relevant for our calculations.

4.3.1. Exact Expressions

The 'exact' expression for the fermionic propagator is given by, [2], [3] and [10],

$$
\begin{aligned}
\left\langle \psi_i(p)\bar{\psi}^j(-q)\right\rangle &= \delta_i^j S(p)\cdot(2\pi)^3\delta^3(p-q)\\
S(q) &\equiv \frac{-i\gamma^\mu q_\mu + i\lambda^2\gamma^+ q^- + \lambda q_s}{q^2}\\
\implies S(q) &= -i\frac{\gamma^+ q^-(1-\lambda^2) + \gamma^- q^+ + \gamma^z q_z + Ii\lambda q_s}{q^2} = -i\frac{R(q)}{q^2}\\
\implies R(q) &= (\gamma^+ q^-(1-\lambda^2) + \gamma^- q^+ + \gamma^z q_z + Ii\lambda q_s)
\end{aligned}
\tag{4.18}
$$

Directing from equation 4.14, the 'exact' expressions for the $\mathcal{O}$, J^+ and J^- operators, which have already been computed by [10], are listed here for convenience.

$$\begin{aligned}
J_0 &= \mathcal{O} = \bar{\psi} V^0 \psi \\
J_1^+ &= J^+ = \bar{\psi} V^+ \psi \\
J_1^- &= J^- = \bar{\psi} V^- \psi
\end{aligned} \tag{4.19}$$

where, V^0, V^- and V^+ are the 'exact' vertices for the corresponding operators.

$$\begin{aligned}
V^+(p,q) &= g^+(y)\gamma^+ + \frac{2q^+}{p} f^+(y) \\
V^-(p,q) &= i\gamma^- + \frac{q_s^2}{2\left(q^+\right)^2} g^-(y)\gamma^+ + \frac{q_s^2}{pq^+} f^-(y) \\
V^0(p,q) &= \frac{\lambda q_s}{q^+} g^0(y)\gamma^+ + f^0(y)
\end{aligned} \tag{4.20}$$

while the complicated functions involved in the 'exact' expressions are,

$$\begin{aligned}
f^+(y) &= \frac{i}{2}\left[1 - e^{2i\hat{\lambda}\left(\tan^{-1}(\Lambda') - \tan^{-1}(y)\right)}\right] \\
g^+(y) &= \frac{i}{2}\left[1 - i\hat{\lambda}y + (1 + i\hat{\lambda}y) e^{2i\hat{\lambda}\left(\tan^{-1}(\Lambda') - \tan^{-1}(y)\right)}\right] \\
f^-(y) &= \frac{i}{2y^2}\left[1 - 2i\hat{\lambda}y - e^{-2i\hat{\lambda}\tan^{-1}(y)}\right] \\
g^-(y) &= \frac{i}{2y^2}\left[(1 + i\hat{\lambda}y) e^{-2i\hat{\lambda}\tan^{-1}(y)} - (1 - i\hat{\lambda}y)\right] \\
f^0(y) &= \frac{1 + e^{-2i\hat{\lambda}\tan^{-1}(y)}}{1 + e^{-2i\hat{\lambda}\tan^{-1}(\Lambda')}} \\
g^0(y) &= \frac{1 - i\hat{\lambda}y - (1 + i\hat{\lambda}y) e^{-2i\hat{\lambda}\tan^{-1}(y)}}{\hat{\lambda}y\left[1 + e^{-2i\hat{\lambda}\tan^{-1}(\Lambda')}\right]} \\
y &= \frac{2q_s}{|p|}, \qquad \Lambda' = \frac{2\Lambda}{|p|}, \qquad \hat{\lambda} = \lambda \cdot \mathrm{sgn}(p)
\end{aligned} \tag{4.21}$$

It is crucial to emphasize that q represents the propagator momenta and p denotes the external momenta. Therefore, with $p = p_z$, the expression $\mathrm{sgn}(p) = \mathrm{sgn}(p_z)$ is meaningful.

4.3.2. All-loop Expressions

Within this section, it is crucial to remember that the findings presented are sourced directly from existing literature, and are presented in their original state. This may lead to confusion due to the various notations and indices used. But, to avoid any ambiguity, we explicitly clarify the relevant notations for each result, emphasizing their relevance within this particular context. Unless mentioned, all the variables follow the natural flow narration in this article.

The complete expressions for the 3-point correlator, $\langle T_{--} J_+ J_+ \rangle$ in the scalar theory coupled with CS theiry, worked out by [16], is expressed in the below.

$$\begin{aligned}
&\langle T_{--}(-q) J_+\left(-q'\right) J_+\left(-q''\right)\rangle \\
&= -\frac{iN}{32\pi\lambda}\frac{1}{qq'q''}\left[e^{-\pi i\hat{\lambda}'}\left(q'^4 - q'^2 q''^2\right) + e^{-\pi i \hat{\lambda}''}\left(q''^4 - q'^2 q''^2\right) + \right. \\
&\qquad \left. q'^2 q''^2 e^{-\pi i\left(\hat{\lambda}'+\hat{\lambda}''\right)} - e^{\pi i\hat{\lambda}} q^4 + q'q''\left(4q'^2 + 7q'q'' + 4q''^2\right) - 12\lambda^2 q'q''q^2\right]
\end{aligned} \tag{4.22}$$

where, q, q' and q'' are the external momenta.

The parity-even and part of $\langle T_{--} J_+ J_+ \rangle$ can be written down as,

$$\begin{aligned}
\langle\cdot\rangle_{\lambda-\text{ even}} = &-\frac{N}{32\pi}\frac{\sin(\pi\lambda)}{\lambda}\left[\left(\frac{|q|^3}{q'q''} + \frac{|q'|^3}{qq''} + \frac{|q''|^3}{qq'}\right)\cos^2\left(\frac{\pi\lambda}{2}\right)\right. \\
&\left. + \left(\frac{|q|^3}{q'q''} + \frac{|q'|^3}{qq''} + \frac{|q''|^3}{qq'} - 2\frac{q''\,|q'| + q'\,|q''|}{q}\right)\sin^2\left(\frac{\pi\lambda}{2}\right)\right]
\end{aligned} \tag{4.23}$$

Similarly, the parity-odd part of $\langle T_{--} J_+ J_+ \rangle$ can be found as,

$$\langle\cdot\rangle_{\lambda-\text{ odd}} = \frac{Ni}{32\pi\lambda}\left[4\left(3\lambda^2 + \cos(\pi\lambda) - 1\right)q + \sin^2(\pi\lambda)\frac{|q'|\,|q''| + q'q''}{q}\right] \tag{4.24}$$

Now, moving towards 4-point correlators, it is quite essential to describe the following notation,

$$\langle \ldots \rangle = \langle\langle \ldots \rangle\rangle (2\pi)^3 \delta^3(\sum_i p_i) \tag{4.25}$$

where, p_i's are the external momenta. The δ denotes the momentum conservation.

The 4-point correlator, $\langle J^+ J^- \mathcal{O}\mathcal{O}\rangle$ in the free fermionic theory coupled with CS theory, worked out by [2], is expressed in the below.

$$\begin{aligned}
&\left\langle\left\langle \tilde{J}^+(p)\tilde{J}^-(q)\tilde{O}(\epsilon)\tilde{O}(\delta)\right\rangle\right\rangle \\
&= \frac{-1}{\tilde{N}\left(1+\tilde{\lambda}^2\right)^2}\left(\left[\frac{1}{4}\frac{q|p|+p|q|+\epsilon|\delta|+\delta|\epsilon|}{(\epsilon+\delta)(q+\epsilon)(q+\delta)}+\frac{1}{4}\frac{-|\delta|-|\epsilon|+|q+\epsilon|+|q+\delta|}{qp}\right]+\right. \\
&i\tilde{\lambda}\left[\frac{(p-q)}{2pq}+\frac{1}{4}\left(\frac{(|q|q+|p|p)\left(p^2-q^2\right)+\left(\epsilon^2+\delta^2\right)(|q|q-|p|p)}{pq(p+\delta)(p+\epsilon)(p+q)}\right)(\operatorname{sgn}(\epsilon)+\operatorname{sgn}(\delta))\right. \\
&\left.+\frac{|p+\epsilon|-|p+\delta|}{4pq}(\operatorname{sgn}(\delta)-\operatorname{sgn}(\epsilon))\right]+\tilde{\lambda}^2\left[\frac{(q|p|+p|q|)\operatorname{sgn}(\epsilon)\operatorname{sgn}(\delta)+\epsilon|\delta|+\delta|\epsilon|}{4(p+\delta)(p+\epsilon)(p+q)}\right. \\
&\left.\left.+\frac{|\epsilon||\delta|(|p+\epsilon|+|p+\delta|)+(|\epsilon|+|\delta|)\epsilon\delta}{4pq\epsilon\delta}+\frac{(q|q|+p|p|)(1+\operatorname{sgn}(\epsilon)\operatorname{sgn}(\delta))}{4pq(\epsilon+\delta)}\right]\right)
\end{aligned} \tag{4.26}$$

where, p, q, ϵ and δ are the external momenta. It is worth mentioning that the notation from equation 3.3 is currently being utilized. Also, we make use of another short notation, (follwoing [2])

$$\begin{aligned}
\tilde{\mathcal{O}} &= \frac{1}{\sqrt{\tilde{N}}(1+\tilde{\lambda}^2)}\mathcal{O} \\
\tilde{J}_s &= \frac{1}{\sqrt{\tilde{N}}}J_s
\end{aligned} \tag{4.27}$$

Now, the relevant parity-even terms are simply the $\tilde{\lambda}^0$ and $\tilde{\lambda}^2$ terms and the parity-odd contributions come from $\tilde{\lambda}$ term.

The detailed expression for $\langle J^+ J^- J^+ J^-\rangle$ in the free fermionic theory coupled with CS theory, can be located in the appendix B of [2]. Due to its extensive nature, the complete expression is not included here.

Chapter 5

Computation and Analysis

Within this section, we present all the computed results and offer a concise overview of the insights gained from each calculation.

5.1. $\langle TJJ \rangle$

Directed from equation 4.23, and using the notations in equation 3.3, we get,

$$\langle \cdot \rangle_{\lambda \text{ even}}$$
$$= \frac{-\tilde{N}}{64(1+\tilde{\lambda}^2)} \left[\left(\frac{|q|^3}{q'q''} + \frac{|q'|^3}{qq''} + \frac{|q''|^3}{qq'} \right) + \left(\frac{|q|^3}{q'q''} + \frac{|q'|^3}{qq''} + \frac{|q''|^3}{qq'} - \frac{2(q''\,|q'| + q'\,|q''|)}{q} \right) \tilde{\lambda}^2 \right] \tag{5.1}$$

Similarly, from equation 4.24, we get,

$$\langle \cdot \rangle_{\lambda \text{ odd}} = \frac{i\tilde{N}\tilde{\lambda}}{64(1+\tilde{\lambda}^2)} \frac{2(|q'|\,|q''| + q'q'')}{q} \tag{5.2}$$

Regarding the parity-odd expression, the initial term can be safely disregarded as it represents a contact term that transforms into a delta function in position space, ensuring no loss of generality in this context. (see [16])

At this point, directly following from equation 3.2 it can be easily checked that,

$$
\begin{aligned}
\langle T_{--}(-q)J_{+}(-q')\,J_{+}(-q'')\rangle_{F.F.} &= \frac{-1}{64}\left(\frac{|q|^3}{q'q''}+\frac{|q'|^3}{qq''}+\frac{|q''|^3}{qq'}-\frac{2(q''\,|q'|+q'\,|q''|)}{q}\right)\\
\langle T_{--}(-q)J_{+}(-q')\,J_{+}(-q'')\rangle_{C.B.} &= \frac{-1}{64}\left(\frac{|q|^3}{q'q''}+\frac{|q'|^3}{qq''}+\frac{|q''|^3}{qq'}\right)\\
\langle T_{--}(-q)J_{+}(-q')\,J_{+}(-q'')\rangle_{\text{Odd}} &= \frac{-i}{32}\,\frac{q'q''[\operatorname{sgn}(q')\operatorname{sgn}(q'')+1]}{q} \qquad \text{and,}
\end{aligned} \tag{5.3}
$$

$$
\begin{aligned}
&\langle T_{--}(-q)J_{+}(-q')\,J_{+}(-q'')\rangle_{\text{F.F.-C.B.}}\\
&= \langle T_{--}(-q)J_{+}(-q')\,J_{+}(-q'')\rangle_{\text{F.F.}} - \langle T_{--}(-q)J_{+}(-q')\,J_{+}(-q'')\rangle_{\text{C.B.}}\\
&= \frac{2(q''\,|q'|+q'\,|q''|)}{64q}\\
&= \frac{q'q''[\operatorname{sgn}(q')+\operatorname{sgn}(q'')]}{32q}
\end{aligned} \tag{5.4}
$$

Now, following from equation 4.8, the epsilon transformation on $\langle T_{--}(-q)J_{+}(-q')\,J_{+}(-q'')\rangle_{\text{F.F.- C.B.}}$ has the following functional form,

$$
\begin{aligned}
&\epsilon\cdot\langle T_{--}(-q)J_{+}(-q')\,J_{+}(-q'')\rangle_{\text{F.F.-C.B.}}\\
&= \epsilon^{-z+}\operatorname{sgn}(-q')\left\langle T_{--}(-q)J^{-}(-q')\,J_{+}(-q'')\right\rangle_{\text{F.F.-C.B.}}\\
&\qquad + \epsilon^{-z+}\operatorname{sgn}(-q'')\left\langle T_{--}(-q)J_{+}(-q')\,J^{-}(-q'')\right\rangle_{\text{F.F.-C.B.}}\\
&= (\operatorname{sgn}(-q')+\operatorname{sgn}(-q''))\,\langle T_{--}(-q)J_{+}(-q')\,J_{+}(-q'')\rangle_{\text{F.F.-C.B.}}\\
&= -(\operatorname{sgn}(q')+\operatorname{sgn}(q''))\times\frac{q'q''[\operatorname{sgn}(q')+\operatorname{sgn}(q'')]}{32q}\\
&= -\frac{q'q''[\operatorname{sgn}(q')\operatorname{sgn}(q'')+1]}{16q}
\end{aligned} \tag{5.5}
$$

Here, it is quite essential to notice that epsilon transformation only acts either on the J vertices or on the T vertex.

Therefore, we find,

$$\epsilon \cdot \langle T_{--}(-q) J_{+}\left(-q^{\prime}\right) J_{+}\left(-q^{\prime \prime}\right)\rangle_{\text{F.F.-C.B.}} = i\,\langle T_{--}(-q) J_{+}\left(-q^{\prime}\right) J_{+}\left(-q^{\prime \prime}\right)\rangle_{\text{Odd}} \tag{5.6}$$

5.2. $\langle JJ\mathcal{O}\mathcal{O}\rangle$

Directly following from equations 3.2, 4.26 and 4.27 and recalling the notations in equation 3.3 and 4.25, the parts of $\langle JJ\mathcal{O}\mathcal{O}\rangle$ are found to be,

$$\begin{aligned}
\left\langle\left\langle \tilde{J}^{+}\tilde{J}^{-}\tilde{O}\tilde{O}\right\rangle\right\rangle_{\text{F.F.}} &= \Bigg[\frac{(q|p|+p|q|)\operatorname{sgn}(\epsilon)\operatorname{sgn}(\delta)+\epsilon|\delta|+\delta|\epsilon|}{4(p+\delta)(p+\epsilon)(p+q)}+ \\
&\qquad \frac{|\epsilon||\delta|(|p+\epsilon|+|p+\delta|)+(|\epsilon|+|\delta|)\epsilon\delta}{4pq\epsilon\delta}+\frac{(q|q|+p|p|)(1+\operatorname{sgn}(\epsilon)\operatorname{sgn}(\delta))}{4pq(\epsilon+\delta)}\Bigg] \\
\left\langle\left\langle \tilde{J}^{+}\tilde{J}^{-}\tilde{O}\tilde{O}\right\rangle\right\rangle_{\text{C.B.}} &= \left[\frac{1}{4}\frac{q|p|+p|q|+\epsilon|\delta|+\delta|\epsilon|}{(\epsilon+\delta)(q+\epsilon)(q+\delta)}+\frac{1}{4}\frac{-|\delta|-|\epsilon|+|q+\epsilon|+|q+\delta|}{qp}\right] \\
\left\langle\left\langle \tilde{J}^{+}\tilde{J}^{-}\tilde{O}\tilde{O}\right\rangle\right\rangle_{\text{Odd}} &= i\Bigg[\frac{(p-q)}{2pq}+\frac{1}{4}\left(\frac{(|q|q+|p|p)\left(p^{2}-q^{2}\right)+\left(\epsilon^{2}+\delta^{2}\right)(|q|q-|p|p)}{pq(p+\delta)(p+\epsilon)(p+q)}\right) \\
&\qquad (\operatorname{sgn}(\epsilon)+\operatorname{sgn}(\delta))+\frac{|p+\epsilon|-|p+\delta|}{4pq}(\operatorname{sgn}(\delta)-\operatorname{sgn}(\epsilon))\Bigg]
\end{aligned} \tag{5.7}$$

where, p, q, ϵ and δ are the associated external momenta with the $J^{+}, J^{-}, \mathcal{O}$ and $\mathcal{O}$ vertices, respectively. Now, the epsilon transformation of $\left\langle\left\langle \tilde{J}^{+}(p)\tilde{J}^{-}(q)\tilde{O}(\epsilon)\tilde{O}(\delta)\right\rangle\right\rangle_{\text{F.F.-C.B.}}$ (following from equation 4.8) gives,

$$\begin{aligned}
&\epsilon\cdot\left\langle\left\langle \tilde{J}^{+}(p)\tilde{J}^{-}(q)\tilde{\mathcal{O}}(\epsilon)\tilde{\mathcal{O}}(\delta)\right\rangle\right\rangle_{\text{F.F.- C.B.}} \\
&=\epsilon^{+z-}\operatorname{sgn}(p)\left\langle\left\langle \tilde{J}_{-}(p)\tilde{J}^{-}(q)\tilde{\mathcal{O}}(\epsilon)\tilde{\mathcal{O}}(\delta)\right\rangle\right\rangle_{\langle\cdots\rangle}+\epsilon^{-z+}\operatorname{sgn}(q)\left\langle\left\langle \tilde{J}^{+}(p)\tilde{J}_{+}(q)\tilde{\mathcal{O}}(\epsilon)\tilde{\mathcal{O}}(\delta)\right\rangle\right\rangle_{\langle\cdots\rangle} \\
&=(\operatorname{sgn}(p)-\operatorname{sgn}(q))\left\langle\left\langle \tilde{J}^{+}(p)\tilde{J}^{-}(q)\tilde{\mathcal{O}}(\epsilon)\tilde{\mathcal{O}}(\delta)\right\rangle\right\rangle_{\text{F.F.- C.B.}}
\end{aligned} \tag{5.8}$$

Now, a deep simplification of these expressions leads to the following relation,

$$(\mathrm{sgn}(p)-\mathrm{sgn}(q))\left\langle\left\langle \tilde{J}^{+}(p)\tilde{J}^{-}(q)\tilde{O}(\epsilon)\tilde{O}(\delta)\right\rangle\right\rangle_{\text{F.F.-C.B.}}+\frac{1}{i}\left\langle\left\langle \tilde{J}^{+}(p)\tilde{J}^{-}(q)\tilde{O}(\epsilon)\tilde{O}(\delta)\right\rangle\right\rangle_{\text{Odd}}=X \quad (5.9)$$

Now using the momentum conservation equation, 4.25, we get the term X to be zero, for all possible physical kinematic regime. Hence,

$$\epsilon\cdot\left\langle\left\langle \tilde{J}^{+}(p)\tilde{J}^{-}(q)\tilde{O}(\epsilon)\tilde{O}(\delta)\right\rangle\right\rangle_{\text{F.F.-C.B.}}=i\left\langle\left\langle \tilde{J}^{+}(p)\tilde{J}^{-}(q)\tilde{O}(\epsilon)\tilde{O}(\delta)\right\rangle\right\rangle_{\text{Odd}} \quad (5.10)$$

5.3. $\langle JJJJ\rangle$

The explicit expression for, $\langle JJJJ\rangle$ as given in the appendix B of [2], has the following form,

$$\begin{aligned}\left\langle\left\langle \tilde{J}^{+}(a)\tilde{J}^{-}(b)\tilde{J}^{+}(c)\tilde{J}^{-}(d)\right\rangle\right\rangle &= \frac{1}{\tilde{N}\left(1+\tilde{\lambda}^{2}\right)}\Big[\left\langle\left\langle \tilde{J}^{+}(a)\tilde{J}^{-}(b)\tilde{J}^{+}(c)\tilde{J}^{-}(d)\right\rangle\right\rangle_{\text{C.B.}} \\ +\tilde{\lambda}\left\langle\left\langle \tilde{J}^{+}(a)\tilde{J}^{-}(b)\tilde{J}^{+}(c)\tilde{J}^{-}(d)\right\rangle\right\rangle_{\text{Odd}} &+\tilde{\lambda}^{2}\left\langle\left\langle \tilde{J}^{+}(a)\tilde{J}^{-}(b)\tilde{J}^{+}(c)\tilde{J}^{-}(d)\right\rangle\right\rangle_{\text{F.F.}}\Big]\end{aligned} \quad (5.11)$$

where, a, b, c and d are the external momenta associated with the J^{+}, J^{-}, J^{+} and J^{-} vertices, respectively. Now, the epsilon transformation gives,

$$\begin{aligned}&\epsilon\cdot\left\langle\left\langle \tilde{J}^{+}(a)\tilde{J}^{-}(b)\tilde{J}^{+}(c)\tilde{J}^{-}(d)\right\rangle\right\rangle_{\text{F.F.-C.B.}}\\ &=\epsilon^{+z-}\,\mathrm{sgn}(a)\left\langle\left\langle \tilde{J}_{-}(a)\tilde{J}^{-}(b)\tilde{J}^{+}(c)\tilde{J}^{-}(d)\right\rangle\right\rangle_{\text{F.F.-C.B.}}\\ &\quad+\epsilon^{-z+}\,\mathrm{sgn}(b)\left\langle\left\langle \tilde{J}^{+}(a)\tilde{J}_{+}(b)\tilde{J}^{+}(c)\tilde{J}^{-}(d)\right\rangle\right\rangle_{\text{F.F.-C.B.}}\\ &\quad+\epsilon^{+z-}\,\mathrm{sgn}(c)\left\langle\left\langle \tilde{J}^{+}(a)\tilde{J}^{-}(b)\tilde{J}_{-}(c)\tilde{J}^{-}(d)\right\rangle\right\rangle_{\text{F.F.-C.B.}}\\ &\quad+\epsilon^{-z+}\,\mathrm{sgn}(d)\left\langle\left\langle \tilde{J}^{+}(a)\tilde{J}^{-}(b)\tilde{J}^{+}(c)\tilde{J}_{+}(d)\right\rangle\right\rangle_{\text{F.F.-C.B.}}\\ &=(\mathrm{sgn}(a)-\mathrm{sgn}(b)+\mathrm{sgn}(c)-\mathrm{sgn}(d))\left\langle\left\langle \tilde{J}^{+}(a)\tilde{J}^{-}(b)\tilde{J}^{+}(c)\tilde{J}^{-}(d)\right\rangle\right\rangle_{\text{F.F.-C.B.}}\end{aligned} \quad (5.12)$$

Hereafter, again using the equation 4.8, we find,

$$(\mathrm{sgn}(a) - \mathrm{sgn}(b) + \mathrm{sgn}(c) - \mathrm{sgn}(d)) \left\langle\left\langle \tilde{J}^{+}(a)\tilde{J}^{-}(b)\tilde{J}^{+}(c)\tilde{J}^{-}(d)\right\rangle\right\rangle_{F.F.-C.B.}$$
$$= i\left\langle\left\langle \tilde{J}^{+}(a)\tilde{J}^{-}(b)\tilde{J}^{+}(c)\tilde{J}^{-}(d)\right\rangle\right\rangle_{Odd} + iY \tag{5.13}$$

Now, using momentum conservation equation 4.25, we came across an interesting result. The Y term is such that when the following condition is satisfied,

$$\mathrm{sgn}(a) = \mathrm{sgn}(c) = -\,\mathrm{sgn}(b) = -\,\mathrm{sgn}(d) \tag{5.14}$$

it becomes exactly equal to the parity-odd term, otherwise it is zero. Basically, when the external momenta associated with the J^{+} vertices are of the same sign but opposite to the sign of the external momenta associated with the J^{-} vertices (here, in our case, the alternate momenta), the extra term becomes,

$$Y = \left\langle\left\langle \tilde{J}^{+}(a)\tilde{J}^{-}(b)\tilde{J}^{+}(c)\tilde{J}^{-}(d)\right\rangle\right\rangle_{Odd} \tag{5.15}$$

Otherwise, the extra term Y is zero.

5.4. T Exact Vertex

One of our objective is to calculate the $TJJ\mathcal{O}$ correlator up to the leading order in 1/N and all orders in the 't Hooft coupling λ. To achieve this, the exact expressions for all vertices and propagators are required. Therefore, obtaining the exact expression for the stress-energy tensor, T (denoted as J_2), is crucial. The methodology for deriving the exact expression for the stress-energy tensor mirrors the approach outlined in [10].

The definition for the T operator is given by,

$$\begin{aligned}
T^{\mu\nu} = J_2^{\mu\nu} &= \bar{\psi}\gamma^{(\mu}D^{\nu)}\psi - (\text{traces}) \\
&= \frac{1}{2!}\bar{\psi}\left[\gamma^{\mu}D^{\nu} + \gamma^{\nu}D^{\mu}\right]\psi - \frac{1}{2!}\bar{\psi}\left[\gamma^{\mu}D^{\nu} + \gamma^{\nu}D^{\mu}\right]\psi g_{\mu\nu} \\
&= \frac{1}{2}\bar{\psi}\left[\gamma^{\mu}\left(\partial^{\nu} - igA^{\nu}\right) + \gamma^{\nu}\left(\partial^{\mu} - igA^{\mu}\right)\right]\psi - \bar{\psi}\gamma^{\mu}D_{\mu}\psi \\
&= -\frac{i}{2}\bar{\psi}\left[\gamma^{\mu}(q^{\nu} + gA^{\nu}) + \gamma^{\nu}(q^{\mu} + gA^{\mu})\right]\psi
\end{aligned} \tag{5.16}$$

Since, we are working on massless limit, the Dirac equation gives, $\bar{\psi}\gamma^{\mu}D_{\mu}\psi = 0$ and the propagator momenta here is depicted by q and p denotes the external momenta. Therefore, the free vertex expression is,

$$V_0^{\mu\nu}(p,q) = -\frac{i}{2}\left[\gamma^{\mu}(q^{\nu} + gA^{\nu}) + \gamma^{\nu}(q^{\mu} + gA^{\mu})\right] \tag{5.17}$$

It is straightforward to see that, $V_0^{\mu\mu}(p,q) = -i\gamma^{\mu}(q^{\mu} + gA^{\mu})$ and $V_0^{\mu\nu}(p,q) = V_0^{\nu\mu}(p,q)$.

Since we are working in the light-cone gauge, $A^+ = A_- = 0$, the free vertex expressions for T^{++}, T^{+-}, T^{-+} and T^{--} are given by,

$$\begin{aligned}
&V_0^{++} = -i\gamma^+ q^+ = -iq_-\gamma^+, \qquad V_0^{--} = -i\gamma^-(q^- + gA^-) = -i(q_+ + gA_+)\gamma^+ \qquad \text{and,} \\
&V_0^{+-} = V_0^{-+} = -\frac{i}{2}\Big[\gamma^+(q^- + gA^-) + \gamma^-(q^+ + gA^+)\Big] = -\frac{i}{2}\Big[\gamma^+(q_+ + gA_+) + \gamma^- q_-\Big]
\end{aligned} \tag{5.18}$$

Now, using equations 4.15 and 4.18, the exact vertex expression can be achieved as,

$$V^{\mu\nu}(p,q) = -\frac{i}{2}\left[\gamma^{\mu}(q^{\nu} + gA^{\nu}) + \gamma^{\nu}(q^{\mu} + gA^{\mu})\right] - 2\pi i\lambda\int\frac{d^3k}{(2\pi)^3}\frac{\gamma^{[3|}R(k)V^{\mu\nu}(p,k)R(k-p)\gamma^{|+]}}{k^2(k-p)^2(q-k)^+} \tag{5.19}$$

where, the updated propagator contributions in the numerator are simply,

$$R(k) = \gamma^+ k^- (1-\lambda^2) + \gamma^- k^+ + \gamma^z k_z + Ii\lambda k_s$$
$$R(k-p) = \gamma^+ k^- (1-\lambda^2) + \gamma^- k^+ + \gamma^z (k_z - p) + Ii\lambda k_s \tag{5.20}$$

(Since, p is the external momenta, only the z-component survives, and $p = p_z$.)

Now considering $R(k)V^{++}(p,k)R(k-p)$ as the A matrix, and following equation 4.16, the relevant parts can be found and the exact vertex expression becomes,

$$V^{\mu\nu}(q,p) = -\frac{i}{2}\left[\gamma^\mu(p^\nu + gA^\nu) + \gamma^\nu(p^\mu + gA^\mu)\right] - 4\pi i\lambda \int \frac{d^3k}{(2\pi)^3} \frac{a_I\gamma^+ - a_- I}{k^2(k-q)^2(q-k)^+} \tag{5.21}$$

$$\text{and,} \qquad R(k)V^{\mu\nu}(p,k)R(k-p) = a_+\gamma^+ + a_-\gamma^- + a_z\gamma^z + a_I I \tag{5.22}$$

5.4.1. Computation of T^{++} vertex

Considering T^{++} vertex, equations 5.21 and 5.22 becomes,

$$V^{++}(p,q) = -i\gamma^+ q^+ + 4\pi i\lambda \int \frac{d^3k}{(2\pi)^3} \frac{a_I\gamma^+ - a_- I}{k^2(k-q)^2(k-p)^+} \tag{5.23}$$

$$\text{and,} \qquad R(k)V^{++}(p,k)R(k-p) = a_+\gamma^+ + a_-\gamma^- + a_z\gamma^z + a_I I \tag{5.24}$$

Now, from 5.23, it is clear that the exact T^{++} vertex cannot have any dependence on γ^- and γ^z. So, we can ansatz the exact expression as the following way,

$$V^{++}(p,q) := v_+(p,q)\gamma^+ + v_I(p,q)I \tag{5.25}$$

Now, implementing equations, 5.20, 5.24 and 5.25 into the exact T^{++} vertex expression, 5.23 and working out a lengthy algebra, produces,

$$
\begin{aligned}
a_I &= (2i\lambda k_s + q_z)k^+ v_+(p,k) + [2k^+k^-(1-\lambda^2) + (k_z+p)k_z - \lambda^2 k_s^2]v_I(p,k) \\
a_- &= 2(k^+)^2 v_+(p,k) + [-pk^+ + 2i\lambda k_s k^+]v_I(p,k)
\end{aligned}
\tag{5.26}
$$

Hence,

$$
\begin{aligned}
v_+(p,q) &= -iq^+ + 4\pi i\lambda \int \frac{d^3k}{(2\pi)^3} \frac{(2i\lambda k_s + p)k^+ v_+(p,q) + [k_s^2(1-2\lambda^2) + (k_z+q_z)k_z]v_I(p,k)}{k^2(k-p)^2(k-q)^+} \\
v_I(p,q) &= -4\pi i\lambda \int \frac{d^3k}{(2\pi)^3} \frac{2(k^+)^2 v_+(p,k) + [-pk^+ + 2i\lambda k_s k^+]v_I(p,k)}{k^2(k-p)^2(k-q)^+}
\end{aligned}
\tag{5.27}
$$

From these equations and depending on the regime we are working for the external momenta, it is quite obvious that $V^{++}(q,p)$ can only depend on q_+, q_- and p. Now, we shift to cylindrical coordinates (k_s, θ, k_z). So, the z-component integral is quite easy to do. After doing this integral, the expressions look like,

$$
\begin{aligned}
v_+(p,q) &= -iq^+ + 4\pi i\lambda \int_0^\infty \frac{k_s dk_s}{2\pi} \int_0^{2\pi} \frac{d\theta}{2\pi} \frac{(2i\lambda k_s + p)k^+ v_+(p,k) + 2k_s^2(1-\lambda^2)v_I(p,k)}{p^2 k_s[1+(2k_s/p)^2](k-q)^+} \\
v_I(p,q) &= -4\pi i\lambda \int_0^\infty \frac{k_s dk_s}{2\pi} \int_0^{2\pi} \frac{d\theta}{2\pi} \frac{2(k^+)^2 v_+(q,k) + [-p + 2i\lambda k_s]k^+ v_I(q,k)}{p^2 k_s[1+(2k_s/p)^2](k-q)^+}
\end{aligned}
\tag{5.28}
$$

Now, checking the tensor structure of these expressions and following from dimensional analysis and rotational invariance in the x-y plane, it is quite easy to guess the functional form as,

$$
\begin{aligned}
& v_+(p,q) := q^+ g(p,q) \qquad v_I(p,q) := \frac{2(q^+)^2}{p} f(p,q) \\
\implies\ & v_+(p,k) := k^+ g(p,k) \qquad v_I(p,k) := \frac{2(k^+)^2}{p} f(p,k)
\end{aligned}
\tag{5.29}
$$

where, $g(p,q)$ and $f(p,q)$ are some functional form which we have to discover. Inserting this updated ansatz, leads to,

$$
\begin{aligned}
q^+ g(p,q) &= -iq^+ + \frac{2i\lambda}{p}\int_0^\infty dk_s \frac{(i\lambda\frac{2k_s}{p}+1)g(p,k)+(\frac{2k_s}{p})^2(1-\lambda^2)f(p,k)}{1+(2k_s/p)^2}\int_0^{2\pi}\frac{d\theta}{2\pi}\frac{(k^+)^2}{(k-q)^+} \\
\frac{2(q^+)^2}{p} f(p,q) &= -\frac{4i\lambda}{p^2}\int_0^\infty dk_s \frac{g(p,k)+[-1+i\lambda(2k_s/p)]f(p,k)}{1+(2k_s/p)^2}\int_0^{2\pi}\frac{d\theta}{2\pi}\frac{(k^+)^3}{(k-q)^+}
\end{aligned}
\tag{5.30}
$$

Here, at this point, we use the identities for the polar integration,

$$
\int_0^\infty dk_s \int_0^{2\pi}\frac{d\theta}{2\pi}\frac{(k^+)^n}{(k-p)^+} = \int_{p_s}^{\Lambda} dk_s (p^+)^{n-1}
$$

(for $n > 0$ and Λ is the cut-off implemented from cut-off regularization)

$$
\int_0^\infty dk_s \int_0^{2\pi}\frac{d\theta}{2\pi}\frac{(k^+)^n}{(k-p)^+} = -\int_0^{p_s} dk_s (p^+)^{n-1} \qquad \text{(for } n \le 0\text{)}
$$

The derivation of these identities are elaborated in the appendix. These identities further simplify,

$$
\begin{aligned}
q^+ g(p,q) &= -iq^+ + i\lambda q^+ \int_{q_s}^{\Lambda} d\left(\frac{2k_s}{p}\right)\frac{(i\lambda(2k_s/p)+1)g(p,k)+(2k_s/p)^2(1-\lambda^2)f(p,k)}{1+(2k_s/p)^2} \\
\frac{2(q^+)^2}{p} f(p,q) &= -\frac{2i\lambda(q^+)^2}{p}\int_{q_s}^{\Lambda} d\left(\frac{2k_s}{p}\right)\frac{g(p,k)+[-1+i\lambda(2k_s/p)]f(p,k)}{1+(2k_s/p)^2}
\end{aligned}
\tag{5.31}
$$

We also take on a few notations, $x = \frac{2k_s}{|p_z|}$, $y = \frac{2q_s}{|p|}$, $\hat{\lambda} = \lambda \cdot \mathrm{sgn}(p)$, $\Lambda' = \frac{2\Lambda}{p}$ and $b = i\hat{\lambda}$. The complicated expressions now become quite simpler in the new notations,

$$
\begin{aligned}
g(y) &= -i + b\int_y^{\Lambda'} dx \frac{(1+b^2)x^2 f(x)+(1+bx)g(x)}{1+x^2} \\
f(y) &= b\int_y^{\Lambda'} dx \frac{(1-bx)f(x)-g(x)}{1+x^2}
\end{aligned}
\tag{5.32}
$$

Now, solving these recursive integral-differential equations, the solutions can be found as,

$$
\begin{aligned}
f(y) &= -\frac{i}{2}\left[1 - e^{2b(tan^{-1}(\Lambda') - tan^{-1}(y))}\right] \\
g(y) &= -i - (1 + by)f(y) = -\frac{i}{2}\left[1 - by + (1 + by)e^{2b(tan^{-1}(\Lambda') - tan^{-1}(y))}\right]
\end{aligned} \tag{5.33}
$$

Following the same procedure as T^{++}, may lead to the exact expressions for T^{+-}, T^{-+} and T^{--} vertices.

5.5. $\langle TJJ\mathcal{O}\rangle$

In this section, we demonstrate the processes to be followed for the complete computation of the $\langle TJJ\mathcal{O}\rangle$ correlator. We begin with, $T^{++}J^{+}J^{+}O$, as the exact expressions for T^{++} is relatively easier to work with.

5.5.1. Computation of $T^{++}J^{+}J^{+}O$

Now that the exact expression for all the T^{++}, J^{+}, J^{+} and O vertices and the exact propagator $S(p)$ are known, it is straight forward to put all the functions into 'ladder' type diagrams as demonstrated in figure 4.8 and then insert into the reverse Schwinger-Dyson equation described in equation 4.13 for the all order expression. But at this point, it is quite cumbersome task to accomplish, as it requires computing the trace algebra of 12 gamma matrices and then simplifying all the contributions by summing, and then, integrating all that giant expression twice. The integration involves various complex terms like $e^{i\hat{\lambda}tan^{-1}(y)}$ and many more. So, it is quite unfortunate that this is a too hard task to complete, at least using Mathematica. And, there is a need of few more simplifications for further progress. That is why, it is very obvious to turn back to the [problem with the 'free' vertices and 'free' propagators. Therefore, we spend some time on calculating the tree level and 1-loop level contributions for this configuration, with the use of free vertices and free propagators.

Tree Level

The relevant diagrams for this configuration can be directed to the figure 4.5 and then fixing the A, B, C and D vertices to T^{++}, J^{+}, J^{+} and $\mathcal{O}$ operators respectively. Now, we start with the first kind of diagram, the ABCDA (anti-clockwise) diagram. And, the tree level can be written down as,

$$= \alpha \int \frac{d^3q}{(2\pi)^3} \frac{tr[(q_+\gamma^+)\not{q}\gamma^+\not{q}_3\gamma^+\not{q}_2\not{q}_1]}{q^2\ q_1^2\ q_2^2\ q_3^2}$$

As usual, q denotes the propagator momenta and the α in the beginning accounts for overall constant factor, which has to be determined at the end of all calculations. Now, working out (i) the trace algebra first, then carefully doing (ii) the addition algebra with the thought in mind that the external momenta have only the z-component nonzero, and then (iii) shifting from light-cone coordinate to cylindrical coordinate, we rewrite the expression as,

$$= \alpha \int_0^\infty \frac{q_s dq_s}{2\pi} \int_0^{2\pi} \frac{d\theta}{2\pi} \int_{-\infty}^\infty \frac{dq_z}{2\pi} \ \frac{8p_2 q_-^4}{q^2\ q_1^2\ q_2^2\ q_3^2} \tag{5.34}$$

Hereafter, it is pretty easy to notice that (iv) the polar integration will simply give this entire expression to be zero, as q_- can be written as $\frac{q_s}{\sqrt{2}}e^{i\theta}$.

Similarly, the ABDCA diagram tree level can be interpreted as,

$$= \alpha \int \frac{d^3q}{(2\pi)^3} \frac{tr[(q_-\gamma^+)\not{q}\gamma^+\not{q}_3\not{q}_2\gamma^+\not{q}_1]}{q^2\ q_1^2\ q_2^2\ q_3^2}$$

Now, the same simplifications done for the ABCDA diagram can be followed here also, and it gives,

$$= \alpha \int_0^\infty \frac{q_s dq_s}{2\pi} \int_0^{2\pi} \frac{d\theta}{2\pi} \int_{-\infty}^\infty \frac{dq_z}{2\pi} \frac{8p_3 q_-^4}{q^2\ q_1^2\ q_2^2\ q_3^2} \tag{5.35}$$

Now, again considering the polar integral, the expression becomes zero.

For the ACBDA diagram, the expression is,

$$= \alpha \int \frac{d^3q}{(2\pi)^3} \frac{tr[(q_- \gamma^+)\not{q}\not{q}_3 \gamma^+ \not{q}_2 \gamma^+ \not{q}_1]}{q^2 \ q_1^2 \ q_2^2 \ q_3^2}$$

Continually, we follow the same procedure, and head towards,

$$= -\alpha \int_0^\infty \frac{q_s dq_s}{2\pi} \int_0^{2\pi} \frac{d\theta}{2\pi} \int_{-\infty}^{\infty} \frac{dq_z}{2\pi} \ \frac{8P_3 q_-^4}{q^2 \ q_1^2 \ q_2^2 \ q_3^2} \tag{5.36}$$

Yet, again, the polar integration makes this expression zero. Moreover, it is quite important to notice that the expression for this configuration of vertices becoming zero is due to the polar integration, hence, the permutation of the J^+ vertices will also produce the same result. Hence, it is worth mentioning that the tree level diagram for the correlator consisting T^{++}, J^+, J^+ and $\mathcal{O}$ operators is simply zero, independent of the configuration chosen.

1-loop Level

Now, we want to compute the one-loop diagrams. The diagrams associated with 1-loop contributions can be redirected to the figures 4.6, 4.7 and 4.8, while fixing the A, B, C and D vertices to T^{++}, J^+, J^+ and $\mathcal{O}$ operators. For all of these diagrams, we again follow the same steps as described for tree level computation.

(i) Write the expression of that particular diagram.

(ii) Simplify the gamma trace algebra.

(iii) Complete the addition algebra of various terms coming from different configurations of gamma traces.

(iv) Shift from light-cone coordinates to cylindrical coordinates.

(v) Compute the polar integral.

But, it is quite shocking to note that all of these diagrams for any permutation of vertices (T^{++}, J^+, J^+ and $\mathcal{O}$) individually becomes zero, all thanks to the polar integral. Hence, the 1-loop level contribution for $T^{++}J^+J^+\mathcal{O}$ is simply zero.

5.5.2. Computation of $T^{+-}J^{+}J^{+}\mathcal{O}$

The exact expression for T^{+-} is going to be way more complex than T^{++}, hence, it is quite obvious that the computation of $T^{+-}J^{+}J^{+}\mathcal{O}$ would be naturally harder than $T^{++}J^{+}J^{+}\mathcal{O}$ with 'exact' vertices and 'exact' propagators. Therefore, we head towards calculating tree level and 1-loop level contributions for $T^{+-}J^{+}J^{+}\mathcal{O}$, but with free vertices and free propagators.

Tree Level

The tree level diagram for $T^{+-}J^{+}J^{+}\mathcal{O}$ can be redirected to the 4.5 diagram, while A, B, C and D vertices can now be considered as T^{+-}, J^{+}, J^{+} and $\mathcal{O}$ operators respectively.

After following all the same steps as demonstrated for $T^{++}J^{+}J^{+}\mathcal{O}$ in 5.5.1, the ABCDA (anti-clockwise) diagram can be expressed as,

$$
\begin{aligned}
&= \alpha \int \frac{d^3q}{(2\pi)^3} \frac{tr[([q^- + gA^-]\gamma^+ + q^+\gamma^-)\not{q}\gamma^+\not{q}_3\gamma^+\not{q}_2\not{q}_1]}{q^2 q_1^2 q_2^2 q_3^2} \\
&\equiv \alpha \int_0^\infty \frac{q_s dq_s}{2\pi} \int_0^{2\pi} \frac{d\theta}{2\pi} \int_{-\infty}^{\infty} \frac{dq_z}{2\pi} \frac{4q_-^2\left[p_2\left(2gA^-q_- + q_s^2\right) + q_z\left(P_1P_2 + q_s^2\right) - \left(P_1 + P_2\right)q_z^2 + q_z^3\right]}{q^2 q_1^2 q_2^2 q_3^2} \\
&\equiv 0
\end{aligned} \tag{5.37}
$$

where, α denotes the overall constant factor to be determined at the end of the calculation. Similarly, the ABDCA (anti-clockwise) diagram can be written down as,

$$
\begin{aligned}
&= \alpha \int \frac{d^3q}{(2\pi)^3} \frac{tr[([q^- + gA^-]\gamma^+ + q^+\gamma^-)\not{q}\gamma^+\not{q}_3\not{q}_2\gamma^+\not{q}_1]}{q^2 q_1^2 q_2^2 q_3^2} \\
&\equiv \alpha \int_0^\infty \frac{q_s dq_s}{2\pi} \int_0^{2\pi} \frac{d\theta}{2\pi} \int_{-\infty}^{\infty} \frac{dq_z}{2\pi} \frac{4p_3q_-^2\left(2gA^-q_- + q_z\left(P_1 - q_z\right) + q_s^2\right)}{q^2 q_1^2 q_2^2 q_3^2} \\
&\equiv 0
\end{aligned} \tag{5.38}
$$

Likewise, the ACBDA diagram simplifies to,

$$
\begin{aligned}
&= \alpha \int \frac{d^3q}{(2\pi)^3} \frac{tr[([q^- + gA^-]\gamma^+ + q^+\gamma^-)\not{q}\not{q}_3\gamma^+\not{q}_2\gamma^+\not{q}_1]}{q^2 q_1^2 q_2^2 q_3^2} \\
&\equiv -\alpha \int_0^\infty \frac{q_s dq_s}{2\pi} \int_0^{2\pi} \frac{d\theta}{2\pi} \int_{-\infty}^{\infty} \frac{dq_z}{2\pi} \frac{4q_-^2\left[2P_3 gA^- q_- + (p_2 + p_3 + q_z)\, q_s^2 + q_z(q_z - P_1)(q_z - P_3)\right]}{q^2 q_1^2 q_2^2 q_3^2} \\
&\equiv 0
\end{aligned} \tag{5.39}
$$

As before, the symmetrization of the J^+ does not affect the result, as it is the polar integral that makes the expressions to become zero. Hence, the tree level contribution for $T^{+-}J^+J^+\mathcal{O}$ is also coming to be zero, for any permutation of the vertices.

1-loop Level

Hereafter, we move to calculate the 1-loop diagrams for $T^{+-}J^+J^+\mathcal{O}$. The diagrams are the same as 4.6, 4.7 and 4.8 for any configurations of the vertices of our interest. Moreover, we follow the same recipe as before in $T^{++}J^+J^+\mathcal{O}$ in 5.5.1 and come to that particular same conclusion, that is, the polar integral makes all the expressions to become zero!

5.6. $\langle \mathcal{O}\mathcal{O}\mathcal{O}\mathcal{O}\mathcal{O} \rangle$

After doing computation of various different correlators we also spend some time in working out some covariant calculation. The simplest operator $\mathcal{O}$ is taken into consideration. But there has been several attempts to compute 4-point correlators of this scalar operator. So, we jump to get the expressions for 5-point correlation function.

As a basic introduction, we first demonstrate the computation for 2-point tree level $\mathcal{O}$ operator.

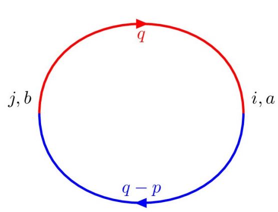

This diagram simplifies to $\frac{|p|}{8}$, where q is the propagator momenta and p is the external momenta.

Figure 5.1: The tree level diagram of the $\mathcal{O}\mathcal{O}$ Operator

Similarly, the tree-level diagram for the 5-point $\mathcal{O}$ operator can be found as,

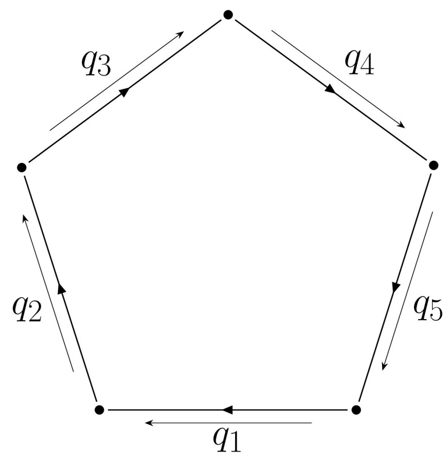

Figure 5.2: The Tree Level 5-point diagram of the $\mathcal{O}$ Operator

which simplifies to,

$$= \int_q \quad i \quad \frac{q_0^\mu \ q_1^\nu \ q_2^\rho \ q_3^\sigma \ q_4^\eta}{q_0^2 \ q_1^2 \ q_2^2 \ q_3^2 \ q_4^2} \quad [\gamma_\mu \gamma_\nu \gamma_\rho \gamma_\sigma \gamma_\eta]^a{}_a \tag{5.40}$$

The trace of gamma matrices include one levi-civita tensor as there are odd numbers of matrices, which means it is a parity-odd contribution, and we can take the liberty to exploit this property and reduce it to a simpler form,

$$= B_1 \left(\int_q \frac{q^\mu}{q_0^2 q_1^2 q_2^2 q_3^2} \right) + B_2(q_3 \rightleftharpoons q_4) + B_3(q_2 \rightleftharpoons q_4) + B_4(q_1 \rightleftharpoons q_4) + B_0(q_0 \rightleftharpoons q_4) \tag{5.41}$$

where, the B's are the corresponding coefficients of the subsequent integrals, which are some complex functions of the external momenta. Now, these integrals can even be simplified to a simpler form, using the 'inversion technique' as demonstrated in [19], [27] and [11] and the 'Schouten Identity' provided in [19] and [28]. These techniques reduce the terms in the denominator but increases the complexity in the numerator, which still remains very complicated, yet these methods are the easiest and effective for the computation of these integrals.

Chapter 6

Results and Discussions

6.1. Results

From the previous chapters, we have listed down the crucial results relevant to our predictions.

6.1.1. Verification of Bosonisation Duality Relations

The computations worked out in this project, clearly validates the applicability of the epsilon transformation over the correlators TJJ and $JJ\mathcal{O}\mathcal{O}$. To put it mathematically,

$$\begin{aligned}
&\langle T_{--}J_+J_+\rangle = A_1\frac{\tilde{N}}{1+\tilde{\lambda}^2}\left[\langle T_{--}J_+J_+\rangle_{\text{C.B.}} + \tilde{\lambda}\,\langle T_{--}J_+J_+\rangle_{\text{Odd}} + \tilde{\lambda}^2\,\langle T_{--}J_+J_+\rangle_{\text{F.F.}}\right] \\
&\text{and} \qquad \epsilon\cdot\left[\langle T_{--}J_+J_+\rangle_{\text{F.F.}} - \langle T_{--}J_+J_+\rangle_{\text{C.B.}}\right] = i\,\langle T_{--}J_+J_+\rangle_{\text{Odd}}
\end{aligned}$$

and,

$$\begin{aligned}
&\left\langle J^+J^-\mathcal{O}\mathcal{O}\right\rangle = A_2\frac{\tilde{N}}{1+\tilde{\lambda}^2}\left[\left\langle J^+J^-\mathcal{O}\mathcal{O}\right\rangle_{\text{C.B.}} + \tilde{\lambda}\left\langle J^+J^-\mathcal{O}\mathcal{O}\right\rangle_{\text{Odd}} + \tilde{\lambda}^2\left\langle J^+J^-\mathcal{O}\mathcal{O}\right\rangle_{\text{F.F.}}\right] \\
&\text{and} \qquad \epsilon\cdot\left[\left\langle J^+J^-\mathcal{O}\mathcal{O}\right\rangle_{\text{F.F.}} - \left\langle J^+J^-\mathcal{O}\mathcal{O}\right\rangle_{\text{C.B.}}\right] = i\left\langle J^+J^-\mathcal{O}\mathcal{O}\right\rangle_{\text{Odd}}
\end{aligned}$$

where, A_1 and A_2 are some overall factors multiplied. Clearly, the epsilon transformation is obeyed up to a factor of $2i$. Hence, the bosonisation duality relations are nicely maintained.

6.1.2. Bosonisation Dualities Relations to Ponder

Now, the epsilon transformation of $JJJJ$ correlator emphasizes,

$$\begin{aligned}
&\left\langle J^+J^-J^+J^-\right\rangle = A_3\frac{\tilde{N}}{1+\tilde{\lambda}^2}\left[\left\langle J^+J^-J^+J^-\right\rangle_{\text{C.B.}} + \tilde{\lambda}\left\langle J^+J^-J^+J^-\right\rangle_{\text{Odd}} + \tilde{\lambda}^2\left\langle J^+J^-J^+J^-\right\rangle_{\text{F.F.}}\right]\\
&\text{and}\qquad \epsilon\cdot\left[\left\langle J^+J^-J^+J^-\right\rangle_{\text{F.F.}} - \left\langle J^+J^-J^+J^-\right\rangle_{\text{C.B.}}\right] = i\left[\left\langle J^+J^-J^+J^-\right\rangle_{\text{Odd}} + Y\right]
\end{aligned}$$

where, the A_3 is some overall factor multiplied. Interestingly, the extra term here appearing, Y is something not observed in the cases of TJJ and $JJ\mathcal{O}\mathcal{O}$. This extra term has the shocking property that, when the opposite external momenta or the external momenta associated with the same kind of helicity operator have the same sign, Y becomes exactly equal to the parity-odd term and otherwise simply becomes zero. In other words,

$$\begin{aligned}
\text{when,}\qquad &\operatorname{sgn}(a) = \operatorname{sgn}(c) = -\operatorname{sgn}(b) = -\operatorname{sgn}(d),\\
&Y = \left\langle J^+(a)J^-(b)J^+(c)J^-(d)\right\rangle_{\text{Odd}}\\
&\text{otherwise,}\qquad Y = 0
\end{aligned}$$

Though the epsilon transformation relation almost gets validity, it is still a good place to investigate for the extra term.

6.1.3. $\langle TJJ\mathcal{O}\rangle$

The most prominent and significant proof for this duality could be provided by the computation of $\langle TJJ\mathcal{O}\rangle$. We have been able to produce a few relevant results regarding this. Exact expressions and loop level contributions for correlators have been computed. We list them here for convenience.

(i) The exact expression for the T^{++} is found to be,

$$T^{++}(p,q) = \overline{\psi}V^{++}(p,q)\psi \qquad \text{and} \qquad V^{++} = \gamma^+ g(y) + If(y)$$

where,

$$
\begin{aligned}
f(y) &= -\frac{i}{2}\left[1 - by + (1+by)e^{2b(\tan^{-1}(\Lambda') - \tan^{-1}(y))}\right] \\
g(y) &= -\frac{i}{2}\left[1 - e^{2b(\tan^{-1}(\Lambda') - \tan^{-1}(y))}\right] \\
y &= \frac{2q_s}{|p|} \qquad \Lambda' = \frac{2\Lambda}{|p|} \\
b &= i\hat{\lambda}, \qquad \hat{\lambda} = \lambda \cdot \mathrm{sgn}(p)
\end{aligned}
$$

while q and p are the propagator momenta and the external momenta, respectively.

(ii) With free vertices and free propagators, the tree level and the 1-loop level contributions for all kinds of configurations of the $T^{++}J^{+}J^{+}\mathcal{O}$ and $T^{+-}J^{+}J^{+}\mathcal{O}$ correlation functions are zero and only for $T^{--}J^{+}J^{+}\mathcal{O}$, the contributions are nonzero.

6.2. Discussions

- As the results summarize, it has very neatly proven the validity of epsilon transformation relation and significantly the applicability of the bosonisation dualities of interest. It strengthens the literature by providing explicit proofs and opens up a broad channel for further works and shows the scope of possible attacks for unraveling the true nature of CFT.
- Although for the $JJJJ$ correlation function, there is a thin cloud of visualization regarding the duality relations, as it even though superficially satisfy the relations, but fails to follow the explicit functional form. Hence, there is much room for further understanding and exploration.
- Bosonisation relations are some very recent developments in the literature. Validating its applicability will solve some stranded problems.
- The exact computation of spin-2 conserved current enriches the theory and help develop the regime. Moreover, the all order calculation can be extensively helpful to understand the underlying field, and it can provide some clues to do the computation covariantly.
- The methods used here can be used as a well demonstrated and summarized tool for doing perturbative calculations efficiently, as here we not only gather techniques of some

previously available methods, but also connect them and create a few more for smoothing the computation work.

- Moreover, the covariant approach made in the end of this project work provide a scope to understand the possible symmetries and compatibility of methods with the actual expressions.

Chapter 7

Conclusion

The Chern-Simons matter theory is a unique subset of Conformal Field Theory, distinguished by its intriguing bosonisation duality relations that establish connections between distinct theories. This project is dedicated to explicitly confirming these relations and outlining potential directions for future exploration. Our approach involves computing various correlation functions of conserved currents and referencing prior research to deepen our understanding. Our primary goal is to validate these bosonisation duality relations, and while we have achieved success in some instances, there are areas where further work is needed. In these cases, we have meticulously outlined the methodologies required to derive the specific expressions of interest. To get through the duality relations, we have computed various correlation functions of conserved currents. These computations not only aid in comprehending the theory but also contribute to its advancement. Throughout our investigation, we have unearthed noteworthy analytical results that enrich the existing literature. Additionally, we have delved into mathematical expressions that facilitate smoother and more efficient computations, enhancing the overall research endeavor.

Hence, our conclusion highlights the potential for validating bosonisation dualities within the Chern-Simons matter theory. It is evident that confirming these dualities necessitates substantial computational efforts, representing a significant undertaking. Streamlining the computational tools can offer profound insights into the theory, as demonstrated in our investigation. While the current status indicates the validity of these relations, further exploration is essential to ascertain their true nature and implications within the theory. This underscores the importance of continued study and analysis to unravel the full extent of these bosonisation dualities and their impact on the Chern-Simons matter theory.

Bibliography

[1] J. Maldacena and A. Zhiboedov, Constraining conformal field theories with a higher spin symmetry, 2011.

[2] R.R. Kalloor, Four-point functions in large n chern-simons fermionic theories, Journal of High Energy Physics **2020** (2020) .

[3] S. Giombi, S. Minwalla, S. Prakash, S.P. Trivedi, S.R. Wadia and X. Yin, Chern–simons theory with vector fermion matter, The European Physical Journal C **72** (2012) .

[4] B. Gabai, A. Sever and D.-l. Zhong, Line operators in chern-simons–matter theories and bosonization in three dimensions, Physical Review Letters **129** (2022) .

[5] G.F. de Teramond, A. Paul, S.J. Brodsky, A. Deur, H.G. Dosch, T. Liu et al., The strong coupling in the nonperturbative and near-perturbative regimes, 2024.

[6] K. Wernli, Lecture notes on chern-simons perturbation theory, 2019.

[7] S. Axelrod and I.M. Singer, Chern-simons perturbation theory, 1991.

[8] G.V. Dunne, Aspects of chern-simons theory, 1999.

[9] G.W. Moore, "Introduction to chern-simons theories." `https://www.physics.rutgers.edu/~gmoore/TASI-ChernSimons-StudentNotes.pdf`, 2019.

[10] G. Gur-Ari and R. Yacoby, Correlators of large n fermionic chern-simons vector models, Journal of High Energy Physics **2013** (2013) .

[11] R. Yacoby, Scalar correlators in bosonic chern-simons vector models, 2018.

[12] S. Jain, R.R. John, A. Mehta and K.S. Dhruva, Constraining momentum space cft correlators with consistent position space ope limit and the collider bound, Journal of High Energy Physics **2022** (2022) .

[13] P. Jain, S. Jain, B. Sahoo, D.K. S and A. Zade, Mapping slightly broken higher spin (sbhs) theory correlators to free theory correlators: A momentum space bootstrap using sbhs symmetry, 2022.

[14] M.R. Gaberdiel, An introduction to conformal field theory, Reports on Progress in Physics **63** (2000) 607–667.

[15] S. Jain and R.R. John, Relation between parity-even and parity-odd cft correlation functions in three dimensions, Journal of High Energy Physics **2021** (2021) .

[16] O. Aharony, G. Gur-Ari and R. Yacoby, Correlation functions of large n chern-simons-matter theories and bosonization in three dimensions, Journal of High Energy Physics **2012** (2012) .

[17] S. Jain, R.R. John, A. Mehta, A.A. Nizami and A. Suresh, Momentum space parity-odd cft 3-point functions, Journal of High Energy Physics **2021** (2021) .

[18] S. Jain, R.R. John and V. Malvimat, Constraining momentum space correlators using slightly broken higher spin symmetry, Journal of High Energy Physics **2021** (2021) .

[19] S. Jain, R.R. John and V. Malvimat, Momentum space spinning correlators and higher spin equations in three dimensions, Journal of High Energy Physics **2020** (2020) .

[20] K. Jensen, A master bosonization duality, Journal of High Energy Physics **2018** (2018) .

[21] T. Heinzl, Light-cone quantization: Foundations and applications, 2000.

[22] Y.-Q. Gu, Light-cone coordinate system in general relativity, 2017.

[23] J.M.F. Labastida and E. Pérez, Kontsevich integral for vassiliev invariants from chern–simons perturbation theory in the light-cone gauge, Journal of Mathematical Physics **39** (1998) 5183–5198.

[24] A. Bedhotiya and S. Prakash, A test of bosonization at the level of four-point functions in chern-simons vector models, Journal of High Energy Physics **2015** (2015) 1–20.

[25] G.J. Turiaci and A. Zhiboedov, Veneziano amplitude of vasiliev theory, Journal of High Energy Physics **2018** (2018) .

[26] K. Inbasekar, S. Jain, S. Mazumdar, S. Minwalla, V. Umesh and S. Yokoyama, Unitarity, crossing symmetry and duality in the scattering of n = 1 $\mathcal{N} = 1$ susy matter chern-simons theories, Journal of High Energy Physics **2015** (2015) .

[27] D. Anninos, F. Denef, R. Monten and Z. Sun, Higher spin de sitter hilbert space, 2017.

[28] J. Smith, W.L. van Neerven and J.A.M. Vermaseren, Transverse mass and width of the w boson, Phys. Rev. Lett. **50** (1983) 1738.

Appendices

Appendix A

Polar Integrals

The polar integral identities can be obtained in the following way,

$$\begin{aligned}
&\int_0^{2\pi}\frac{d\theta}{2\pi}\frac{(k^+)^n}{(k-p)^+} && \text{(for, } |n|\geq 1 \text{ integer)}\\
&=\int_0^{2\pi}\frac{d\theta}{2\pi}(k^+)^{n-1}+(p^+)\int_0^{2\pi}\frac{d\theta}{2\pi}\frac{(k^+)^{n-1}}{(k-p)^+}\\
&=(p^+)\int_0^{2\pi}\frac{d\theta}{2\pi}\frac{(k^+)^{n-1}}{(k-p)^+} && \text{(Since, } k^+=\tfrac{k_s}{\sqrt{2}}e^{+i\theta} \text{ and, } \textstyle\int_0^{2\pi}\frac{d\theta}{2\pi}e^{in\theta}=0)
\end{aligned}$$

Therefore, for $n \geq 1$

$$\begin{aligned}
\int_0^{2\pi}\frac{d\theta}{2\pi}\frac{(k^+)^n}{(k-p)^+} &= (p^+)\int_0^{2\pi}\frac{d\theta}{2\pi}\frac{(k^+)^{n-1}}{(k-p)^+} = (p^+)^2\int_0^{2\pi}\frac{d\theta}{2\pi}\frac{(k^+)^{n-2}}{(k-p)^+} = \cdots\\
&= (p^+)^{n-1}\int_0^{2\pi}\frac{d\theta}{2\pi}\frac{k^+}{(k-p)^+}
\end{aligned}$$

Therefore, for $n \leq -1$

$$\int_0^{2\pi}\frac{d\theta}{2\pi}\frac{1}{(k^+)^n(k-p)^+} = \frac{1}{(p^+)}\int_0^{2\pi}\frac{d\theta}{2\pi}\frac{1}{(k^+)^{n-1}(k-p)^+} = \frac{1}{(p^+)^2}\int_0^{2\pi}\frac{d\theta}{2\pi}\frac{1}{(k^+)^{n-2}(k-p)^+}$$
$$= \cdots = \frac{1}{(p^+)^{n-1}}\int_0^{2\pi}\frac{d\theta}{2\pi}\frac{1}{k^+(k-p)^+}$$
$$\equiv \frac{1}{(p^+)^n}\int_0^{2\pi}\frac{d\theta}{2\pi}\frac{1}{(k-p)^+} \tag{A.1}$$

Now,

$$\begin{aligned}
&\int_0^{2\pi}\frac{d\theta}{2\pi}\frac{k^+}{(k-p)^+} \\
&= \int_0^{2\pi}\frac{d\theta}{2\pi}\frac{k_s e^{i\theta}}{k_s e^{i\theta}-p^+} \\
&= \frac{1}{2\pi i}\oint\frac{dz}{z-p^+} && \text{(where, } z = k_s e^{i\theta}\text{)} \\
&= 1 \quad \text{if} \quad z > p^+ \\
\mathit{or}, &= 0 \quad \text{if} \quad z \le p^+ && \text{(Using Cauchy's Residue Thorem)} \\
&\equiv 1 \quad \text{if} \quad k_s > p_s \\
\mathit{or}, &\equiv 0 \quad \text{if} \quad k_s \le p_s && \text{(Using, } 2zz^* \ \ge \text{ (or, } \le\text{)} \, 2p^+p^-\text{)}
\end{aligned}$$

Hence, it is straight forward to achieve,

$$\begin{aligned}
&\int_0^{2\pi}\frac{d\theta}{2\pi}\frac{1}{(k-p)^+} \\
&= \frac{1}{(p^+)}\left[\int_0^{2\pi}\frac{d\theta}{2\pi}\frac{k^+}{(k-p)^+} - \int_0^{2\pi}\frac{d\theta}{2\pi}\right] \\
&\equiv 0 \quad \text{if} \quad k_s > p_s \\
\mathit{or}, &\equiv -\frac{1}{p^+} \quad \text{if} \quad k_s \le p_s
\end{aligned}$$

$$\begin{aligned}
\int_0^{2\pi}\frac{d\theta}{2\pi}\frac{(k^+)^n}{(k-p)^+} &= (p^+)^{n-1} \quad \text{if} \quad k_s > p_s \\
&= 0 \quad \text{if} \quad k_s \le p_s \\
&\qquad \text{(for } n \ge 1\text{)} \\
\int_0^{2\pi}\frac{d\theta}{2\pi}\frac{(k^+)^n}{(k-p)^+} &= 0 \quad \text{if} \quad k_s > p_s \\
&= -(p^+)^{n-1} \quad \text{if} \quad k_s \le p_s \\
&\qquad \text{(for } n \le 0\text{)}
\end{aligned} \tag{A.2}$$

Appendix B

1-loop Calculation Simplifications

The manipulations, shown in Appendix A, can be used to simplify the 1-loop calculations in the following way.

$$\int_0^\infty \frac{dk_s}{2\pi}\int_0^{2\pi}\frac{d\theta}{2\pi}\frac{(k^+)^n}{(k-p)^+} = \int_{p_s}^\infty \frac{dk_s}{2\pi}(p^+)^{n-1} \qquad \text{(for } n \geq 1)$$
$$\int_0^\infty \frac{dk_s}{2\pi}\int_0^{2\pi}\frac{d\theta}{2\pi}\frac{(k^+)^n}{(k-p)^+} = -\int_0^{p_s} \frac{dk_s}{2\pi}(p^+)^{n-1} \qquad \text{(for } n \leq 0)$$

$$\int_0^\infty \frac{dq_s}{2\pi}\int_0^{2\pi}\frac{d\theta_q}{2\pi}\int_0^\infty \frac{dk_s}{2\pi}\int_0^{2\pi}\frac{d\theta_k}{2\pi}\frac{(k^+)^n}{(q^+)^m(q-k)^+} = -\int_0^\infty \frac{dq_s}{2\pi}\int_0^{2\pi}\frac{d\theta_q}{2\pi}\int_{q_s}^\infty \frac{dk_s}{2\pi}(q^+)^{n-1-m} \qquad \text{(for } n \text{ and } m > 0)$$
$$\int_0^\infty \frac{dq_s}{2\pi}\int_0^{2\pi}\frac{d\theta_q}{2\pi}\int_0^\infty \frac{dk_s}{2\pi}\int_0^{2\pi}\frac{d\theta_k}{2\pi}\frac{(q^+)^n}{(k^+)^m(q-k)^+} = \int_0^\infty \frac{dq_s}{2\pi}\int_0^{2\pi}\frac{d\theta_q}{2\pi}\int_0^{q_s} \frac{dk_s}{2\pi}(q^+)^{n-1-m} \qquad \text{(for } n \text{ and } m \leq 0)$$

Clearly, these integrals do not vanish only when, $n-m-1=0$ condition is satisfied. This restricts the polar integrals to two certain forms. Now, if this condition is obeyed, the results are given as,

$$\int_0^\infty \frac{dq_s}{2\pi}\int_0^{2\pi}\frac{d\theta_q}{2\pi}\int_0^\infty \frac{dk_s}{2\pi}\int_0^{2\pi}\frac{d\theta_k}{2\pi}\frac{(k^+)^n}{(q^+)^m(q-k)^+} = -\int_0^\infty \frac{dq_s}{2\pi}\int_{q_s}^\infty \frac{dk_s}{2\pi} \qquad \text{(for } n \text{ and } m > 0\text{)}$$

$$\int_0^\infty \frac{dq_s}{2\pi}\int_0^{2\pi}\frac{d\theta_q}{2\pi}\int_0^\infty \frac{dk_s}{2\pi}\int_0^{2\pi}\frac{d\theta_k}{2\pi}\frac{(q^+)^n}{(k^+)^m(q-k)^+} = \int_0^\infty \frac{dq_s}{2\pi}\int_0^{q_s} \frac{dk_s}{2\pi} \qquad \text{(for } n \text{ and } m \leq 0\text{)}$$